Flavor puzzle in three-Higgs-doublet models: Insights from Branco-Grimus-Lavoura and lessons from flavor data

Dipankar Das,[1,*] Miguel Levy,[2,†] and Anugrah M. Prasad[1,‡]

[1]*Indian Institute of Technology (Indore), Khandwa Road, Simrol, Indore 453 552, India*
[2]*Departement Physik, Universität Basel, Klingelbergstrasse 82, CH-4056 Basel, Switzerland*

(Received 17 March 2025; accepted 18 June 2025; published 21 July 2025)

We study a variant of the three-Higgs-doublet model (3HDM), referred to as the Branco-Grimus-Lavoura–(BGL-)3HDM, incorporating a $U(1)_1 \times U(1)_2$ symmetry, which can distinguish the primary sources of mass for different fermion generations. In the version considered here, the Yukawa matrices in the down-quark and charged lepton sectors are diagonal, thereby eliminating tree-level flavor changing neutral currents (FCNCs) in these sectors. FCNC interactions mediated by neutral nonstandard Higgses are confined to the up-quark sector only. No new Beyond-Standard-Model parameters are introduced by the Yukawa sector of the model, making it as economical as the natural flavor conservation (NFC) versions of 3HDM with a $U(1)_1 \times U(1)_2$ symmetry in terms of the number of free parameters. However, even in the down-quark and in the charged lepton sectors, flavor diagonal but nonuniversal Higgs couplings set this model apart from the NFC versions of the 3HDM.

DOI: 10.1103/hf9s-g762

I. INTRODUCTION

Three-Higgs-doublet models (3HDMs) have been known to be quite useful in the context of flavor model building, especially when used in conjunction with discrete symmetries. Such constructions are generally accompanied by flavor changing neutral currents (FCNCs) mediated by nonstandard scalars. Therefore, one would usually require such nonstandard scalars to be much heavier than the electroweak scale to mitigate the constraints from flavor data. To circumvent this situation, 3HDMs with natural flavor conservation (NFC) [1] have seen a recent surge in popularity [2–4].

In this article, instead of shunning the FCNCs altogether, we contemplate the possibility to disentangle the sources of masses for the different generations of fermions. Quite evidently, generation wise strong mass hierarchies in the fermion sector can then be deferred to some extent to hierarchies among the vacuum expectation values (VEVs) of the three doublets. Admittedly, many efforts have already been made along these directions [5,6], but the resulting models still contain FCNCs controlled by new unknown parameters arising from the Yukawa sector. While the constraints arising from the FCNC couplings in the up-quark sector can be slightly forgiving, we definitely need to be more circumspect about the FCNCs in the down-quark sector. On this note, there exist variants of 3HDMs known as the Branco-Grimus-Lavoura (BGL)-type 3HDM (BGL-3HDM), where the FCNC interactions are limited to a particular sector of fermions [7–10]. In the present work, we study the constructional details of such a BGL-3HDM which accommodates the following list of features:

(i) The textures of the Yukawa matrices should make it apparent that the charged fermions of a particular generation primarily receive their masses from a particular Higgs doublet. As a result, the strong mass hierarchy among the different generations of fermions can be somewhat attributed to a strong VEV hierarchy, $v_1 \ll v_2 \ll v_3$ among the three scalar doublets.

(ii) For the particular variant of the BGL-3HDM considered here, the down-quark and the charged-lepton sectors do not contain FCNC couplings mediated by neutral scalars. Although the neutral Higgs couplings in these sectors are flavor diagonal, they are flavor nonuniversal. This aspect of the model may be exploited to selectively enhance or suppress the nonstandard Higgs couplings with fermions of a desired flavor.

(iii) All the FCNCs, in the up-type BGL-3HDM, occur exclusively in the up-quark sector, with their effects being primarily controlled by the elements of the Cabibbo–Kobayashi–Maskawa (CKM) matrix. This

*Contact author: d.das@iiti.ac.in
†Contact author: miguelpissarra.levy@unibas.ch
‡Contact author: anugrahmprasad@gmail.com

Published by the American Physical Society under the terms of the Creative Commons Attribution 4.0 International license. Further distribution of this work must maintain attribution to the author(s) and the published article's title, journal citation, and DOI. Funded by SCOAP³.

is the feature that carries reminiscence of the BGL-type constructions [11,12].

(iv) Because of the above two features, the constraints arising from the flavor data are quite relaxed to the extent that nonstandard particles with masses below the tera-electron-volt (TeV) scale can successfully pass through the flavor constraints if we do not insist on a very strong hierarchy, $v_1 \ll v_2 \ll v_3$, among the VEVs.

(v) The model is, at the very least, as economical as the NFC versions of 3HDMs in terms of the number of physical parameters. It is quite intriguing to note that this model, despite having a relatively more involved Yukawa sector, does not introduce any new parameters in the Yukawa sector compared to what we already have for 3HDMs with NFC. Therefore, when compared with the NFC avatars of 3HDMs, the predictive abilities are not being compromised.

All of these features can be incorporated within a 3HDM framework when a $U(1) \times U(1)$ symmetry is applied in a "horizontal" manner.[1]

Our current article is organized as follows. In Sec. II we discuss the main features of the model. We also provide the necessary details about the scalar and Yukawa sectors of the model. In Sec. III we analyze the constraints arising from the flavor data. Our main findings are summarized in Sec. IV.

II. THE BGL-3HDM

The model is based on a 3HDM structure, endowed with a global $U(1)_1 \times U(1)_2$ horizontal symmetry, under which the fields transform as

$$U(1)_1:\ (Q_L)_1 \to e^{-i\psi_1}(Q_L)_1, \qquad (n_R)_1 \to e^{-2i\psi_1}(n_R)_1, \qquad \phi_1 \to e^{i\psi_1}\phi_1, \tag{1a}$$

$$U(1)_2:\ (Q_L)_2 \to e^{-i\psi_2}(Q_L)_2, \qquad (n_R)_2 \to e^{-2i\psi_2}(n_R)_2, \qquad \phi_2 \to e^{i\psi_2}\phi_2, \tag{1b}$$

where $Q_L = (p_L n_L)^T$ are the usual Standard Model, (SM) quark $SU(2)_L$ doublets, n_R are the down-type $SU(2)_L$ quark singlets, and the subscripts for the fermionic fields refer to the different generations. For completeness, we also show below the transformations of the lepton fields

$$U(1)_1:\ (L_L)_1 \to e^{-i\psi_1}(L_L)_1, \qquad (\ell_R)_1 \to e^{-2i\psi_1}(\ell_R)_1, \tag{2a}$$

$$U(1)_2:\ (L_L)_2 \to e^{-i\psi_2}(L_L)_2, \qquad (\ell_R)_2 \to e^{-2i\psi_2}(\ell_R)_2, \tag{2b}$$

where, again, $L_L = (\nu_L \ell_L)^T$ are the lepton $SU(2)_L$ doublets and ℓ_R are the $SU(2)_L$ charged lepton singlets.[2] All other remaining fields transform trivially under the flavor symmetry. Just by a quick inspection of the transformation properties of the fields, it is already obvious that the different $U(1)$ symmetries distinguish between the different generations. Indeed, only fermions of the first and second generations are charged under $U(1)_1$ and $U(1)_2$, respectively, justifying their labeling.

It is worth mentioning that the flavor symmetry employed here does not follow the usual prescriptions that are found in NFC models, which distinguish the different sectors. This makes different Higgs doublets to be responsible for the masses of different *types* of fermions [2–4]. In contrast, as we will see shortly, all Higgs doublets here will couple to both up- and down-type quarks.

A. Scalar sector

We first study the scalar sector of the theory. This will be useful in setting up the notations that are used throughout the paper.

Taking into account the field transformations of Eq. (1), the scalar potential can be written as follows [13,14]:

$$\begin{aligned} V_{U(1)\times U(1)} = {} & m_{11}^2\phi_1^\dagger\phi_1 + m_{22}^2\phi_2^\dagger\phi_2 + m_{33}^2\phi_3^\dagger\phi_3 \\ & - (m_{12}^2\phi_1^\dagger\phi_2 + m_{13}^2\phi_1^\dagger\phi_3 + m_{23}^2\phi_2^\dagger\phi_3 + \text{H.c.}) \\ & + \lambda_1(\phi_1^\dagger\phi_1)^2 + \lambda_2(\phi_2^\dagger\phi_2)^2 + \lambda_3(\phi_3^\dagger\phi_3)^2 \\ & + \lambda_4(\phi_1^\dagger\phi_1)(\phi_2^\dagger\phi_2) + \lambda_5(\phi_1^\dagger\phi_1)(\phi_3^\dagger\phi_3) \\ & + \lambda_6(\phi_2^\dagger\phi_2)(\phi_3^\dagger\phi_3) + \lambda_7(\phi_1^\dagger\phi_2)(\phi_2^\dagger\phi_1) \\ & + \lambda_8(\phi_1^\dagger\phi_3)(\phi_3^\dagger\phi_1) + \lambda_9(\phi_2^\dagger\phi_3)(\phi_3^\dagger\phi_2), \end{aligned} \tag{3}$$

where m_{12}^2, m_{13}^2, and m_{23}^2 break the global $U(1)_1 \times U(1)_2$ symmetry softly. The soft-breaking parameters are required to prevent the occurrence of massless pseudoscalars as well as to ensure safe decoupling of the nonstandard scalars [15,16]. We also assume that all the potential parameters (including VEVs) are real.

After the electroweak symmetry breaking, it is convenient to express the scalar doublets in terms of component fields as

$$\phi_k = \begin{pmatrix} w_k^+ \\ \frac{1}{\sqrt{2}}(v_k + h_k + iz_k) \end{pmatrix} \quad \text{with} \qquad k = 1, 2, 3, \tag{4}$$

[1] It is worth noting that the original version in Ref. [7] employed a Z_8 symmetry.

[2] We have not included right-handed neutrinos. Thus, neutrinos are massless in this version of the model just as in the SM. However, if needed, the right-handed neutrinos can be introduced, which will be singlets under both the $SU(2)_L \times U(1)_Y$ gauge symmetry as well as the $U(1)_1 \times U(1)_2$ global symmetry. As a result, small masses for the left-handed neutrinos can easily be generated via the type-I seesaw mechanism.

where $\langle\phi_k\rangle = v_k/\sqrt{2}$ denotes the VEV of the kth doublet. The individual VEVs are further parametrized as follows:

$$v_1 = v\cos\beta_1\cos\beta_2, \qquad v_2 = v\sin\beta_1\cos\beta_2,$$
$$v_3 = v\sin\beta_2, \tag{5}$$

with $v = \sqrt{v_1^2 + v_2^2 + v_3^2} = 246$ GeV being the total electroweak VEV. The detailed analysis of the scalar potential containing the minimization of the potential and diagonalization of the mass matrices can be found in Appendix A.

For later convenience, we choose to work in a Higgs basis [17–19], obtained by rotating the fields in the Lagrangian basis as follows:

$$\begin{pmatrix} H_0 \\ R_1 \\ R_2 \end{pmatrix} = O_\beta \begin{pmatrix} h_1 \\ h_2 \\ h_3 \end{pmatrix}, \qquad \begin{pmatrix} G^0 \\ A_1' \\ A_2' \end{pmatrix} = O_\beta \begin{pmatrix} z_1 \\ z_2 \\ z_3 \end{pmatrix},$$
$$\begin{pmatrix} G^\pm \\ H_1'^\pm \\ H_2'^\pm \end{pmatrix} = O_\beta \begin{pmatrix} w_1^\pm \\ w_2^\pm \\ w_3^\pm \end{pmatrix}, \tag{6}$$

with

$$O_\beta = \begin{pmatrix} \cos\beta_2\cos\beta_1 & \cos\beta_2\sin\beta_1 & \sin\beta_2 \\ -\sin\beta_1 & \cos\beta_1 & 0 \\ -\cos\beta_1\sin\beta_2 & -\sin\beta_1\sin\beta_2 & \cos\beta_2 \end{pmatrix}. \tag{7}$$

In Eq. (6), G^0 and $G^\pm$ stand for the neutral and charged Goldstone bosons, respectively. The rest of the fields are not the physical mass eigenstates, in general. However, it should be noted that the state H_0 will have SM-like couplings with the SM particles at the tree level. The physical eigenstates in the mass basis can be obtained via

$$\begin{pmatrix} G^\pm \\ H_1^\pm \\ H_2^\pm \end{pmatrix} = O_{\gamma_2} \begin{pmatrix} G^\pm \\ H_1'^\pm \\ H_2'^\pm \end{pmatrix}, \qquad \begin{pmatrix} G^0 \\ A_1 \\ A_2 \end{pmatrix} = O_{\gamma_1} \begin{pmatrix} G^0 \\ A_1' \\ A_2' \end{pmatrix},$$
$$\begin{pmatrix} h \\ H_1 \\ H_2 \end{pmatrix} = O_\alpha O_\beta^T \begin{pmatrix} H_0 \\ R_1 \\ R_2 \end{pmatrix}, \tag{8}$$

with O_{γ_1}, O_{γ_2}, and O_α defined in Eqs. (A5), (A11), and (A16). Further details can be found in Appendix A.

For the CP-even sector, the field H_0 coincides with the physical mass eigenstate, h, with mass m_h in the *alignment limit* [20] specified by the relations

$$\alpha_1 = \beta_1 \quad \text{and} \quad \alpha_2 = \beta_2. \tag{9}$$

Thus, in this limit, the physical eigenstate, h, mimics the SM Higgs boson in its tree-level couplings with the SM particles. In what follows, we will work in the alignment limit so that the constraints from the Higgs signal strengths [21] are automatically satisfied. However, it should be noted that even in the alignment limit the angle α_3 in O_α is still a free parameter. The main inspiration behind the Higgs basis in Eq. (6) is that the Yukawa couplings have relatively simpler forms in this basis as we will describe in the next subsection.

B. Yukawa sector

Following the standard conventions, we write the Yukawa Lagrangian as

$$\mathscr{L}_Y = -\sum_{k=1}^{3} [\bar{Q}_L\Gamma_k\phi_k n_R + \bar{Q}_L\Delta_k\tilde{\phi}_k p_R + \bar{L}_L\Xi_k\phi_k\ell_R] + \text{H.c.}, \tag{10}$$

where p_R are the up-type quark $SU(2)_L$ singlets and we have suppressed the flavor indices (Γ_k, Δ_k, and Ξ_k are 3×3 matrices in the flavor space). Also, $\tilde{\phi}_k = i\tau_2\phi_k^*$, as usual, with τ_2 being the second Pauli matrix. The mass matrices for the down-type quarks, up-type quarks, and charged leptons are then given by

$$M_n = \frac{1}{\sqrt{2}}\sum_{k=1}^{3} v_k\Gamma_k, \qquad M_p = \frac{1}{\sqrt{2}}\sum_{k=1}^{3} v_k\Delta_k,$$
$$M_\ell = \frac{1}{\sqrt{2}}\sum_{k=1}^{3} v_k\Xi_k. \tag{11}$$

The textures of Γ, Δ, and Ξ matrices that follow from the transformations of Eqs. (1) and (2) are given below:

$$\Gamma_1 = \begin{pmatrix} y_1^d & 0 & 0 \\ 0 & 0 & 0 \\ 0 & 0 & 0 \end{pmatrix}, \qquad \Gamma_2 = \begin{pmatrix} 0 & 0 & 0 \\ 0 & y_2^d & 0 \\ 0 & 0 & 0 \end{pmatrix},$$
$$\Gamma_3 = \begin{pmatrix} 0 & 0 & 0 \\ 0 & 0 & 0 \\ 0 & 0 & y_3^d \end{pmatrix}, \tag{12a}$$

$$\Delta_1 = \begin{pmatrix} a_1 & b_1 & c_1 \\ 0 & 0 & 0 \\ 0 & 0 & 0 \end{pmatrix}, \qquad \Delta_2 = \begin{pmatrix} 0 & 0 & 0 \\ a_2 & b_2 & c_2 \\ 0 & 0 & 0 \end{pmatrix},$$
$$\Delta_3 = \begin{pmatrix} 0 & 0 & 0 \\ 0 & 0 & 0 \\ a_3 & b_3 & c_3 \end{pmatrix}, \tag{12b}$$

$$\Xi_1 = \begin{pmatrix} y_1^\ell & 0 & 0 \\ 0 & 0 & 0 \\ 0 & 0 & 0 \end{pmatrix}, \qquad \Xi_2 = \begin{pmatrix} 0 & 0 & 0 \\ 0 & y_2^\ell & 0 \\ 0 & 0 & 0 \end{pmatrix},$$
$$\Xi_3 = \begin{pmatrix} 0 & 0 & 0 \\ 0 & 0 & 0 \\ 0 & 0 & y_3^\ell \end{pmatrix}. \tag{12c}$$

An intriguing feature already emerges from these textures. Since Γ_k, Ξ_k, and consequently M_n and M_ℓ are already diagonal, it is evident that the masses of each generation in the down-quark and charged lepton sectors will be governed by the VEV of a dedicated scalar doublet. Furthermore, if the VEVs of the scalars are hierarchical ($v_1 \ll v_2 \ll v_3$), the hierarchical structure of the Yukawa coefficients in the down-quark and charged lepton sectors will be significantly diluted.

Although less immediately apparent than in the down-quark sector, it can be demonstrated that the same VEV hierarchy will have analogous effects in the up-quark sector. Specifically, the VEV of a particular scalar doublet will serve as the primary source of mass for each generation of quarks in the up-quark sector as well. Further details on the up-quark sector can be found in Sec. II C. For now, however, we will focus on the FCNC couplings that arise.

To understand the structure of the FCNCs, let us first determine the couplings of the physical quarks to the scalar fields defined in Eq. (6). The couplings to the physical eigenstates can then be easily derived through appropriate rotations originating solely from the scalar sector. To begin with, let us define the physical quark fields via the following unitary rotations:

$$d_L = \mathcal{U}_d n_L, \qquad d_R = \mathcal{V}_d n_R, \qquad u_L = \mathcal{U}_u p_L,$$
$$u_R = \mathcal{V}_u p_R, \qquad e_L = \mathcal{U}_\ell \ell_L, \qquad e_R = \mathcal{V}_\ell \ell_R, \tag{13}$$

where $u \equiv (uct)^T$, $d \equiv (dsb)^T$, and $e \equiv (e\mu\tau)^T$ denote the physical fermion fields. After these rotations, the diagonal mass matrices will be obtained as follows:

$$D_d = \mathcal{U}_d \cdot M_n \cdot \mathcal{V}_d^\dagger = \mathrm{diag}(m_d, m_s, m_b), \tag{14a}$$

$$D_u = \mathcal{U}_u \cdot M_p \cdot \mathcal{V}_u^\dagger = \mathrm{diag}(m_u, m_c, m_t), \tag{14b}$$

$$D_\ell = \mathcal{U}_\ell \cdot M_\ell \cdot \mathcal{V}_\ell^\dagger = \mathrm{diag}(m_e, m_\mu, m_\tau), \tag{14c}$$

and the CKM matrix will be given by $V = \mathcal{U}_u \mathcal{U}_d^\dagger$. Since $M_{n,\ell}$ are already diagonal, we can take $\mathcal{U}_{d,\ell}$ to be the identity matrices, whereas it is understood that $\mathcal{V}_{d,\ell}$ will provide the necessary rephasings such that the elements of $D_{d,\ell}$ are real and positive. Thus, since we are already in a basis where the down-sector is diagonal, we may write

$$\frac{1}{\sqrt{2}} \sum_{k=1}^{3} v_k \Gamma_k = \frac{1}{\sqrt{2}} \mathrm{diag}(v_1 y_1^d, v_2 y_2^d, v_3 y_3^d)$$
$$= \mathrm{diag}(m_d, m_s, m_b). \tag{15}$$

Consequently, the CKM mixing arises exclusively from the up-sector as follows:

$$V = \mathcal{U}_u \cdot \mathcal{U}_d^\dagger \equiv \mathcal{U}_u. \tag{16}$$

With this insight, let us first focus on the neutral Higgs couplings in the CP-even sector. We start with the relevant part of the Yukawa Lagrangian:

$$-\mathscr{L}_{\mathrm{Y}}^{CP-\mathrm{even}} = \frac{1}{\sqrt{2}} \sum_{k=1}^{3} [\bar{n}_L \Gamma_k h_k n_R + \bar{p}_L \Delta_k h_k p_R] + \mathrm{H.c.}$$
$$\equiv \bar{d}_L \left(\frac{1}{\sqrt{2}} \sum_{k=1}^{3} \Gamma_k h_k \right) d_R$$
$$+ \bar{u}_L \mathcal{U}_u \left(\frac{1}{\sqrt{2}} \sum_{k=1}^{3} \Delta_k h_k \right) \mathcal{V}_u^\dagger u_R + \mathrm{H.c.} \tag{17}$$

Using the definitions of Eq. (6), we can decompose h_k as

$$h_k = (O_\beta)_{1k} H_0 + (O_\beta)_{2k} R_1 + (O_\beta)_{3k} R_2, \tag{18}$$

so that the Yukawa Lagrangian in the CP-even sector may be rewritten as

$$-\mathscr{L}_{\mathrm{Y}}^{CP-\mathrm{even}} = \frac{H_0}{\sqrt{2}} \left[\bar{d}_L \left(\sum_{k=1}^{3} (O_\beta)_{1k} \Gamma_k \right) d_R + \bar{u}_L \mathcal{U}_u \left(\sum_{k=1}^{3} (O_\beta)_{1k} \Delta_i \right) \mathcal{V}_u^\dagger u_R \right]$$
$$+ \frac{R_1}{\sqrt{2}} \left[\bar{d}_L \left(\sum_{k=1}^{3} (O_\beta)_{2k} \Gamma_k \right) d_R + \bar{u}_L \mathcal{U}_u \left(\sum_{k=1}^{3} (O_\beta)_{2k} \Delta_k \right) \mathcal{V}_u^\dagger u_R \right]$$
$$+ \frac{R_2}{\sqrt{2}} \left[\bar{d}_L \left(\sum_{k=1}^{3} (O_\beta)_{3k} \Gamma_k \right) d_R + \bar{u}_L \mathcal{U}_u \left(\sum_{k=1}^{3} (O_\beta)_{3k} \Delta_k \right) \mathcal{V}_u^\dagger u_R \right] + \mathrm{H.c.} \tag{19}$$

By virtue of being a Higgs basis, the couplings of H_0 with the physical quarks simplify to

$$-\mathscr{L}_{\mathrm{Y}}^{H^0} = \frac{H_0}{v}[\bar{d}_L D_d d_R + \bar{u}_L D_u u_R] + \mathrm{H.c.} = \frac{H_0}{v}[\bar{d} D_d d + \bar{u} D_u u], \tag{20}$$

elucidating the fact that H_0 has SM-like couplings. This is a general feature of 3HDMs and this is why the constraints from the Higgs-signal strengths are satisfied in the alignment limit.

Since the model does not guarantee the simultaneous diagonalizability of all Yukawa matrices in the up-quark sector, the nonstandard neutral scalars will exhibit tree-level FCNC interactions with the up-type quarks. In fact, the quark couplings of R_1 and R_2 can be easily read from Eq. (19) as

$$\begin{aligned}-\mathscr{L}_{\mathrm{Y}}^{R_i} &= R_1[\bar{d}_L N_1^d d_R + \bar{u}_L N_1^u u_R] \\ &\quad + R_2[\bar{d}_L N_2^d d_R + \bar{u}_L N_2^u u_R] + \mathrm{H.c.} \\ &= R_1[\bar{d}(N_1^d P_R + N_1^{d\dagger} P_L) d \\ &\quad + \bar{u}(N_1^u P_R + N_1^{u\dagger} P_L) u] \\ &\quad + R_2[\bar{d}(N_2^d P_R + N_2^{d\dagger} P_L) d \\ &\quad + \bar{u}(N_2^u P_R + N_2^{u\dagger} P_L) u],\end{aligned} \tag{21}$$

where we have introduced the following shorthand for the matrices that govern the neutral current interactions in the quark Yukawa sectors [7]:

$$N_1^d = \frac{1}{\sqrt{2}}\sum_{k=1}^{3}(O_\beta)_{2k}\Gamma_k,$$

$$N_1^u = \mathcal{U}_u\left(\frac{1}{\sqrt{2}}\sum_{k=1}^{3}(O_\beta)_{2k}\Delta_k\right)\mathcal{V}_u^\dagger, \tag{22a}$$

$$N_2^d = \frac{1}{\sqrt{2}}\sum_{k=1}^{3}(O_\beta)_{3k}\Gamma_k,$$

$$N_2^u = \mathcal{U}_u\left(\frac{1}{\sqrt{2}}\sum_{k=1}^{3}(O_\beta)_{3k}\Delta_k\right)\mathcal{V}_u^\dagger. \tag{22b}$$

Before examining the specific forms of these matrices, we note that the basis choice in Eq. (6) acts on the scalar doublets as a whole. Consequently, these same matrices will also govern the couplings of quarks with the CP-odd and charged scalars, albeit through different combinations. To see this explicitly in the pseudoscalar sector, we use Eq. (6) to write

$$z_k = (O_\beta)_{1k} G_0 + (O_\beta)_{2k} A_1' + (O_\beta)_{3k} A_2'. \tag{23}$$

Following the same steps as in the case of the CP-even sector, we can write the pseudoscalar Yukawa couplings as follows[3]:

$$\begin{aligned}-\mathscr{L}_{\mathrm{Y}}^{CP-\mathrm{odd}} &= \frac{1}{\sqrt{2}}\sum_{k=1}^{3}[\bar{n}_L \Gamma_k (iz_k) n_R - \bar{p}_L \Delta_k (iz_k) p_R] + \mathrm{H.c.} \\ &= iA_1'[\bar{d}(N_1^d P_R - N_1^{d\dagger} P_L) d \\ &\quad - \bar{u}(N_1^u P_R - N_1^{u\dagger} P_L) u] \\ &\quad + iA_2'[\bar{d}(N_2^d P_R - N_2^{d\dagger} P_L) d \\ &\quad - \bar{u}(N_2^u P_R - N_2^{u\dagger} P_L) u].\end{aligned} \tag{24}$$

Finally, Yukawa interactions for the charged scalars can be extracted in a similar manner as follows:

$$\begin{aligned}-\mathscr{L}_{\mathrm{Y}}^{\mathrm{charged}} &= \sqrt{2} H_1'^{+}[\bar{u}(V N_1^d P_R - N_1^{u\dagger} V P_L) d] \\ &\quad + \sqrt{2} H_2'^{+}[\bar{u}(V N_2^d P_R - N_2^{u\dagger} V P_L) d] + \mathrm{H.c.}\end{aligned} \tag{25}$$

C. Up-type quark masses in the BGL-3HDM

Given the textures of the Yukawa matrices, it is natural to wonder how these relate to the physical fermionic masses and mixings. Here, we will sketch the details of how some of the hierarchies in the quark masses and mixings can be transferred to the scalar sector. For an intuitive understanding of the procedure, we have assumed all the Yukawa parameters to be real. However, we have also checked that the phase of the CKM matrix can be easily accommodated once we allow the relevant parameters to be complex.

First, we focus on the down-quark sector due to its simplicity. From Eq. (15), we can readily determine that the Yukawa coefficients necessary for the down-type masses are[4]

$$y_1^d = \frac{\sqrt{2} m_d}{v_1}, \qquad y_2^d = \frac{\sqrt{2} m_s}{v_2}, \qquad y_3^d = \frac{\sqrt{2} m_b}{v_3}. \tag{26}$$

Then, to reduce hierarchies among the Yukawas to the greatest extent, we must have $v_1 \ll v_2 \ll v_3$. For simplicity, define two small parameters, ϵ_1 and ϵ_2[5]:

$$v_1 = \epsilon_1 \epsilon_2 v_3, \qquad v_2 = \epsilon_2 v_3. \tag{27}$$

On the other hand, the up-sector needs to account for both the up-type masses, as well as for the observed quark

[3]The Goldstone Yukawa couplings take the same form as those in the Standard Model and are not explicitly shown here.

[4]The Yukawa couplings (y_k^ℓ) in the charged lepton sector will have similar expressions.

[5]For small values of $\epsilon_{1,2}$, we will have $\tan\beta_1 = 1/\epsilon_1$ and $\tan\beta_2 \approx 1/\epsilon_2$.

mixing. Using Eq. (11) in conjunction with the textures of Δ_i in Eq. (12b), we can write

$$M_p = \frac{1}{\sqrt{2}} \begin{pmatrix} a_1 v_1 & b_1 v_1 & c_1 v_1 \\ a_2 v_2 & b_2 v_2 & c_2 v_2 \\ a_3 v_3 & b_3 v_3 & c_3 v_3 \end{pmatrix}, \tag{28}$$

such that the relevant Hermitian combination is given by

$$\begin{aligned} H_u &= M_p M_p^\dagger \\ &= \frac{1}{2} \begin{pmatrix} v_1^2(a_1^2+b_1^2+c_1^2) & v_1 v_2(a_1 a_2+b_1 b_2+c_1 c_2) & v_1 v_3(a_1 a_3+b_1 b_3+c_1 c_3) \\ . & v_2^2(a_2^2+b_2^2+c_2^2) & v_2 v_3(a_2 a_3+b_2 b_3+c_2 c_3) \\ . & . & v_3^2(a_3^2+b_3^2+c_3^2) \end{pmatrix} \equiv \frac{1}{2} \begin{pmatrix} v_1^2 y_{11} & v_1 v_2 y_{12} & v_1 v_3 y_{13} \\ . & v_2^2 y_{22} & v_2 v_3 y_{23} \\ . & . & v_3^2 y_{33} \end{pmatrix}, \end{aligned} \tag{29}$$

where, for simplicity, we have defined

$$y_{jk} = (a_j a_k + b_j b_k + c_j c_k), \quad \text{with} \quad j,k = 1,2,3. \tag{30}$$

It should be emphasized that these y_{jk}'s are the parameters of physical interest. Our goal is to show that even with this slightly more involved mass squared matrix, the VEVs v_1, v_2, and v_3 remain the dominant sources of masses for m_u, m_c, and m_t, respectively. First, note that for $v_1 \ll v_2 \ll v_3$ and nonhierarchical y_{jk}, the matrix in Eq. (29) is approximately diagonal. In this way, we can anticipate that the rotation angles necessary to bring H_u in its diagonal form are small. This also suggests that the hierarchies in the quark mixing angles can be traced back to the hierarchy of the VEVs. To explore this in greater detail, we will reverse-engineer the matrix H_u from the observed values of quark masses and mixings and express its elements as powers of the Wolfenstein parameter, $\lambda \approx 0.22$. We will then compare this reverse-engineered form of H_u with the expression derived in Eq. (29).

To begin with, we use Eqs. (14) and (16) to write

$$H_u = V^\dagger D_u^2 V, \tag{31}$$

with V being the CKM matrix. To ensure perfect unitarity of the CKM matrix, we use the standard parametrization:

$$V = \mathcal{R}_{23} \cdot \mathcal{R}_{13} \cdot \mathcal{R}_{12}, \tag{32a}$$

with

$$\mathcal{R}_{12} = \begin{pmatrix} c_{\theta_{12}} & s_{\theta_{12}} & 0 \\ -s_{\theta_{12}} & c_{\theta_{12}} & 0 \\ 0 & 0 & 1 \end{pmatrix}, \quad \mathcal{R}_{13} = \begin{pmatrix} c_{\theta_{13}} & 0 & e^{-i\delta} s_{\theta_{13}} \\ 0 & 1 & 0 \\ -e^{i\delta} s_{\theta_{13}} & 0 & c_{\theta_{13}} \end{pmatrix}, \quad \mathcal{R}_{23} = \begin{pmatrix} 1 & 0 & 0 \\ 0 & c_{\theta_{23}} & s_{\theta_{23}} \\ 0 & -s_{\theta_{23}} & c_{\theta_{23}} \end{pmatrix}, \tag{32b}$$

where we denote $c_x \equiv \cos x$, $s_x \equiv \sin x$, and $t_x \equiv \tan x$, throughout the paper. For an intuitive understanding, we will ignore the small CP-violating phase, and therefore we will set $\delta \approx 0$. To make the connection with the Wolfenstein parametrization [22] apparent, one should identify [23]

$$\sin\theta_{12} = \lambda, \qquad \sin\theta_{23} = A\lambda^2, \qquad \sin\theta_{13} = A\lambda^3 \rho. \tag{33}$$

With our objective in mind, we define

$$y_u \lambda^7 = \frac{\sqrt{2} m_u}{v}, \qquad y_c \lambda^3 = \frac{\sqrt{2} m_c}{v}, \qquad y_t = \frac{\sqrt{2} m_t}{v}, \tag{34}$$

with λ being the Wolfenstein expansion parameter, such that $y_{u,c,t} \sim \mathcal{O}(1)$.

Finally, using Eqs. (33) and (34), we find

$$V^\dagger D_u^2 V \approx \frac{v^2}{2}\begin{pmatrix} A^2\lambda^6(1+\rho)^2 y_t^2 & -A^2\lambda^5(1+\rho)y_t^2 & -A\lambda^3(1+\rho)y_t^2 \\ -A^2\lambda^5(1+\rho)y_t^2 & A^2\lambda^4 y_t^2 & A\lambda^2 y_t^2 \\ -A\lambda^3(1+\rho)y_t^2 & A\lambda^2 y_t^2 & y_t^2 \end{pmatrix}, \tag{35}$$

where we have kept only the leading order terms in λ.

Now, combining Eqs. (27) and (29) we may write

$$H_u = \frac{v_3^2}{2}\begin{pmatrix} \epsilon_1^2\epsilon_2^2 y_{11} & \epsilon_1\epsilon_2^2 y_{12} & \epsilon_1\epsilon_2 y_{13} \\ . & \epsilon_2^2 y_{22} & \epsilon_2 y_{23} \\ . & . & y_{33} \end{pmatrix}, \tag{36}$$

where $v_3 \approx v$ will be assumed whenever ϵ_1, $\epsilon_2 \ll 1$ holds true. In fact, looking at Eq. (31) and comparing Eqs. (35) and (36), we can indeed infer that it is desirable to have

$$\epsilon_1 \sim \mathcal{O}(\lambda), \qquad \epsilon_2 \sim \mathcal{O}(\lambda^2), \tag{37}$$

resulting in the hierarchy $v_1 \ll v_2 \ll v_3$.[6]

At this point, it is important to discuss the significance of Eq. (37) in the context of Eqs. (35) and (36). By comparing H_u and $V^\dagger D_u^2 V$, we observe that even if the coefficients y_{jk} are of the similar order, the quark mixing angles will approximately match the experimentally measured values due to the hierarchical structure of the VEVs. Therefore, the Yukawa coefficients in this model do not need to conspire among themselves to account for the smallness of the mixing angles, in contrast to the situation in the SM.

To obtain the physical masses in the up-sector, we need to proceed perturbatively. The top mass can be extracted by simply comparing the leading terms of the (3, 3) elements in Eqs. (35) and (36):

$$y_t^2 v^2 \approx y_{33} v_3^2. \tag{38}$$

Thus, using Eq. (34), we can write

$$m_t \equiv \frac{1}{\sqrt{2}} y_3^u v_3, \quad \text{with} \quad y_3^u = \sqrt{y_{33}}, \tag{39}$$

which implies that v_3 will be the dominant source for the mass of top quark.

From Eq. (35), it is clear that all the leading contributions to H_u stem from the top Yukawa. As such, extracting the charm (and up) Yukawas will not be as straightforward. In fact, doing so requires going beyond the leading order in λ. To extract the charm quark mass we need to focus on the (2, 2), (2, 3), and (3, 3) elements of $(V^\dagger D_u^2 V)$ in Eq. (35), and keep terms up to $\mathcal{O}(\lambda^6)$:

$$\frac{2}{v^2}(V^\dagger D_u^2 V)_{3,3} = y_t^2 - A^2\lambda^4 y_t^2 - A^2\lambda^6\rho^2 y_t^2 + \mathcal{O}(\lambda^{10}), \tag{40a}$$

$$\frac{2}{v^2}(V^\dagger D_u^2 V)_{2,2} = A^2\lambda^4 y_t^2 + \lambda^6(y_c^2 - A^2(1+2\rho)y_t^2) + \mathcal{O}(\lambda^8), \tag{40b}$$

$$\frac{2}{v^2}(V^\dagger D_u^2 V)_{2,3} = A\lambda^2 y_t^2 - A\lambda^4\left(\frac{1}{2}+\rho\right)y_t^2 - A\left(\frac{1}{8}+\frac{A^2}{2}\right)\lambda^6 y_t^2 + \mathcal{O}(\lambda^8). \tag{40c}$$

Inspecting Eq. (40b), we can see that at this order in λ, we already have the influence of the charm Yukawa. Moreover, noticing the similarity of the leading terms of Eqs. (40b) and (40c), we can isolate it by exploiting

$$(V^\dagger D_u^2 V)_{3,3}(V^\dagger D_u^2 V)_{2,2} - (V^\dagger D_u^2 V)_{2,3}^2 \approx \frac{v^4}{4}[\lambda^6 y_c^2 y_t^2 + \mathcal{O}(\lambda^8)]. \tag{41}$$

Similar to the approach used for Eq. (38), we can compare this with the corresponding combination of elements in Eq. (36) to obtain the leading order contribution to y_c:

$$\frac{v^4}{4}\lambda^6 y_c^2 y_t^2 \approx (H_u)_{3,3}(H_u)_{2,2} - (H_u)_{2,3}^2, \tag{42a}$$

$$\Rightarrow y_c^2 \approx \frac{v_3^4}{v^4}\frac{\epsilon_2^2}{\lambda^6}\frac{y_{22}y_{33} - y_{23}^2}{y_t^2}. \tag{42b}$$

Now using Eq. (34) in conjunction with Eqs. (27) and (39) we can write the charm quark mass as follows:

$$m_c \equiv \frac{1}{\sqrt{2}} y_2^u v_2, \quad \text{with} \quad y_2^u = \sqrt{\frac{y_{22}y_{33} - y_{23}^2}{y_{33}}}, \tag{43}$$

which should make obvious the fact that v_2 is the dominant source of m_c. Finally, we need to estimate the mass of the up quark. The simplest way to do it will be to note from Eq. (31) that

[6]One should note that such a hierarchy, although desirable, may not be essential. We can easily see this in the limit $V = 1$ which is not very far from reality. In this limit, Eq. (31) reduces to simply $H_u \equiv D_u^2$. Therefore, comparison with Eq. (36) will lead to $y_{jk} = 0$ for $j \neq k$, and $m_u^2 = y_{11}\epsilon_1^2\epsilon_2^2 v_3^2 \equiv y_{11}v_1^2$, $m_c^2 = y_{22}\epsilon_2^2 v_3^2 \equiv y_{22}v_2^2$, and $m_t^2 = y_{33}v_3^2$ clearly depicting the segregation of the sources of masses for the different generations of up-type quarks.

$$\mathrm{Det}(H_u) = \mathrm{Det}(D_u^2) \equiv m_u^2 m_c^2 m_t^2. \tag{44}$$

Using Eq. (36) we can easily calculate

$$\mathrm{Det}(H_u) = \frac{1}{8} v_3^6 \epsilon_1^2 \epsilon_2^4 f(y_{jk}), \tag{45a}$$

$$\text{with} \quad f(y_{jk}) = [y_{11}(y_{22}y_{33} - y_{23}^2) - y_{12}^2 y_{33} + 2y_{12}y_{13}y_{23} - y_{13}^2 y_{22}]. \tag{45b}$$

Now we can use Eq. (44) together with Eqs. (39), (43), and (27) to obtain

$$m_u \equiv \frac{1}{\sqrt{2}} y_1^u v_1, \quad \text{with} \quad y_1^u = \sqrt{\frac{f(y_{jk})}{y_{22}y_{33} - y_{23}^2}}. \tag{46}$$

Thus collecting Eqs. (39), (43), and (46) together we can write the diagonal mass matrix in the up-quark sector in a form analogous to Eq. (15)

$$\frac{1}{\sqrt{2}} \mathrm{diag}(v_1 y_1^u, v_2 y_2^u, v_3 y_3^u) = \mathrm{diag}(m_u, m_c, m_t). \tag{47}$$

D. Structures of the neutral current matrices

Since the matrices $N_{1,2}^{u,d}$ defined in Eq. (22) govern the Yukawa couplings of the nonstandard scalars, it is important to investigate the detailed structures of these matrices. As we will show, these matrices in this model are fully determined in terms of the quark masses and mixings and $\tan\beta_{1,2}$ [7].

Since the Yukawa matrices in the down-quark sector are diagonal from the very beginning, the forms of $N_{1,2}^d$ are particularly simple. Plugging the textures of Eq. (15) into the definitions of Eq. (22) and then using the explicit form of O_β in Eq. (7), we can easily find

$$N_1^d = \mathrm{diag}\left(\frac{m_d (O_\beta)_{21}}{v_1}, \frac{m_s (O_\beta)_{22}}{v_2}, \frac{m_b (O_\beta)_{23}}{v_3}\right) = \mathrm{diag}\left(-\frac{m_d}{v}\frac{t_{\beta_1} t_{\beta_2}}{s_{\beta_2}}, \frac{m_s}{v}\frac{t_{\beta_2}}{t_{\beta_1} s_{\beta_2}}, 0\right), \tag{48a}$$

$$N_2^d = \mathrm{diag}\left(\frac{m_d (O_\beta)_{31}}{v_1}, \frac{m_s (O_\beta)_{32}}{v_2}, \frac{m_b (O_\beta)_{33}}{v_3}\right) = \mathrm{diag}\left(-\frac{m_d}{v} t_{\beta_2}, -\frac{m_s}{v} t_{\beta_2}, \frac{m_b}{v}\frac{1}{t_{\beta_2}}\right). \tag{48b}$$

Clearly, the down-quark sector does not exhibit any tree-level FCNCs mediated by the nonstandard scalars. Furthermore, while the nonstandard neutral Higgs couplings are flavor diagonal in the down-quark sector, they are not flavor universal. To elucidate this feature further, we can define a parameter [24]

$$\mathcal{F}_k^q = \frac{(N_k^d)_{qq}}{m_q}, \tag{49}$$

with $k = 1, 2$ and $q = d, s, b$. Unlike in the NFC versions of 3HDMs, the value of the quantity $\mathcal{F}_k^q$ will crucially depend on the flavor, q, as can be explicitly checked using Eq. (48). This characteristic can be utilized, for instance, to selectively enhance the coupling strengths of the second-generation fermions relative to those with the third generation. As already explained, these flavor nonuniversal couplings distinguish the current model from the corresponding NFC versions of 3HDMs.

Let us now proceed to find the neutral current matrices in the up-quark sector. To do that, we first explicitly define the following projection matrices:

$$P_1 = \mathrm{diag}(1,0,0), \qquad P_2 = \mathrm{diag}(0,1,0), \qquad P_3 = \mathrm{diag}(0,0,1). \tag{50}$$

From Eqs. (12b) and (11) we can then write (no summation over k)

$$\Delta_k = \frac{\sqrt{2}}{v_k} P_k \cdot M_p, \quad \text{for } k = 1,2,3. \tag{51}$$

Substituting this into the definition of N_1^u in Eq. (22a) and then using Eq. (14), we get

$$N_1^u = \mathcal{U}_u \left(\sum_{k=1}^{3} \frac{(O_\beta)_{2k}}{v_k} P_k M_p\right) \mathcal{V}_u^\dagger = \sum_{k=1}^{3} \frac{(O_\beta)_{2k}}{v_k} \mathcal{U}_u P_k M_p \mathcal{V}_u^\dagger = \sum_{k=1}^{3} \frac{(O_\beta)_{2k}}{v_k} \mathcal{U}_u P_k \mathcal{U}_u^\dagger D_u. \tag{52}$$

Now we can use Eq. (16) to write (no summation over k)

$$(\mathcal{U}_u P_k \mathcal{U}_u^\dagger D_u)_{ab} \equiv (V P_k V^\dagger D_u)_{ab} = (V)_{ak} (V)_{bk}^* (D_u)_{bb}. \tag{53}$$

Using this we can express the elements of N_1^u in a simple form as follows:

$$(N_1^u)_{ab} = \sum_{k=1}^{3} \frac{(O_\beta)_{2k}}{v_k} (V)_{ak} (V)_{bk}^* (D_u)_{bb} = \left(\frac{-t_{\beta_1} t_{\beta_2}}{s_{\beta_2}} (V)_{a1} (V)_{b1}^* + \frac{t_{\beta_2}}{t_{\beta_1} s_{\beta_2}} (V)_{a2} (V)_{b2}^*\right) \frac{(D_u)_{bb}}{v}, \tag{54a}$$

where the explicit form of D_u has been given in Eq. (14). Following similar steps, the elements of N_2^u will be given by[7]

$$(N_2^u)_{ab} = \sum_{k=1}^{3} \frac{(O_\beta)_{3k}}{v_k} (V)_{ak} (V)^*_{bk} (D_u)_{bb}$$
$$= \left(-t_{\beta_2} (V)_{a1} (V)^*_{b1} - t_{\beta_2} (V)_{a2} (V)^*_{b2} + \frac{1}{t_{\beta_2}} (V)_{a3} (V)^*_{b3} \right) \frac{(D_u)_{bb}}{v}. \quad (54b)$$

For the sake of completeness, we also provide the explicit expressions for the neutral current matrices in the charged lepton sector, which will resemble $N_{1,2}^d$ in Eq. (48) and are given by

$$N_1^\ell = \mathrm{diag}\left(\frac{m_e (O_\beta)_{21}}{v_1}, \frac{m_\mu (O_\beta)_{22}}{v_2}, \frac{m_\tau (O_\beta)_{23}}{v_3}, \right)$$
$$= \mathrm{diag}\left(-\frac{m_e}{v} \frac{t_{\beta_1} t_{\beta_2}}{s_{\beta_2}}, \frac{m_\mu}{v} \frac{t_{\beta_2}}{t_{\beta_1} s_{\beta_2}}, 0 \right), \quad (55a)$$

$$N_2^\ell = \mathrm{diag}\left(\frac{m_e (O_\beta)_{31}}{v_1}, \frac{m_\mu (O_\beta)_{32}}{v_2}, \frac{m_\tau (O_\beta)_{33}}{v_3}, \right)$$
$$= \mathrm{diag}\left(-\frac{m_e}{v} t_{\beta_2}, -\frac{m_\mu}{v} t_{\beta_2}, \frac{m_\tau}{v} \frac{1}{t_{\beta_2}} \right). \quad (55b)$$

It should be emphasized that the expressions for the matrices $N_{1,2}^{u,d,\ell}$ in Eqs. (48), (54), and (55) are completely general and valid for any values of $\tan\beta_{1,2}$. Therefore, although the hierarchy $v_1 \ll v_2 \ll v_3$ is desirable from an aesthetic viewpoint, it is not essential for the phenomenological viability of the model. In fact, in Fig. 1 we have displayed the region in the $\tan\beta_1$-$\tan\beta_2$ plane consistent with the perturbativity of the nonstandard Yukawa couplings, $|(N_{1,2}^{u,d,\ell})_{ab}| \leq \sqrt{4\pi}$. As shown in Fig. 1, the benchmark sample ($\tan\beta_1 = 5$, $\tan\beta_2 = 25$), which is compatible with the hierarchy $v_1 \ll v_2 \ll v_3$, lies toward the boundary of the perturbative regime, where the Yukawa couplings of the nonstandard scalars are presumably large and of $\mathcal{O}(1)$. Therefore, for such values of $\tan\beta_{1,2}$, flavor constraints are expected to impose strong bounds on the nonstandard masses. As a result, portions of the allowed parameter space in Fig. 1 will be excluded once flavor constraints are applied. As we will see in the next section, the exact extent to which the allowed region in Fig. 1 shrinks due to the flavor constraints will depend crucially on how light the nonstandard masses that we wish to accommodate are.

[7]It may be noted that, in the limit $V = 1$, the expressions of $N_{1,2}^u$ in Eq. (54) take the same form as those of $N_{1,2}^d$ in Eq. (48).

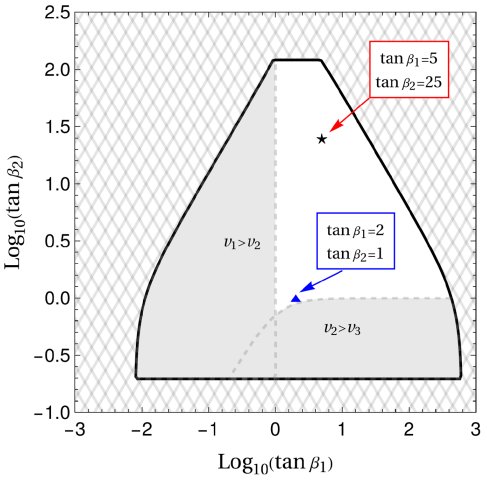


FIG. 1. Allowed regions from the perturbativity constraints on the Yukawa couplings. The crossed-out area outside the black boundary denotes the combined region forbidden by the constraint $|(N_{1,2}^{u,d,\ell})_{ab}| \leq \sqrt{4\pi}$. The shaded areas inside the boundary on the left and on the bottom right denote the regions in which the VEV hierarchies invert: $v_1 > v_2$ (left) and $v_2 > v_3$ (bottom right). The benchmark value $\tan\beta_1 \approx \mathcal{O}(1/\lambda) \approx 5$ and $\tan\beta_2 \approx \mathcal{O}(1/\lambda^2) \approx 25$ is marked with a star, and is inspired from Eq. (37). We also show with a blue triangle the benchmark $\tan\beta_1 = 2$ and $\tan\beta_2 = 2$, in which the VEV hierarchies are relaxed.

III. CONSTRAINTS FROM FLAVOR DATA

The severity of the constraints on the nonstandard masses from the flavor data will depend on how strongly the nonstandard scalars couple to the SM fermions, especially the quarks. Since the Yukawa couplings are completely determined if we specify $\tan\beta_{1,2}$, we provide the magnitudes of the elements of $N_{1,2}^{u,d}$ for two sets of benchmark values of $\tan\beta_{1,2}$. For the benchmark ($\tan\beta_1 = 5$, $\tan\beta_2 = 25$) implying $v_1 \approx 2$ GeV, $v_2 \approx 10$ GeV, and $v_3 \approx 246$ GeV we have

$$|N_1^d| \approx \begin{pmatrix} 2.54\times10^{-3} & 0 & 0 \\ 0 & 2.03\times10^{-3} & 0 \\ 0 & 0 & 0 \end{pmatrix}, \quad (56a)$$

$$|N_2^d| \approx \begin{pmatrix} 5.08\times10^{-4} & 0 & 0 \\ 0 & 1.02\times10^{-2} & 0 \\ 0 & 0 & 6.83\times10^{-4} \end{pmatrix}, \quad (56b)$$

$$|N_1^u| \approx \begin{pmatrix} 9.64\times10^{-4} & 1.51\times10^{-1} & 7.63\times10^{-1} \\ 2.32\times10^{-4} & 8.37\times10^{-3} & 6.98\times10^{-2} \\ 8.85\times10^{-6} & 5.26\times10^{-4} & 5.32\times10^{-4} \end{pmatrix}, \quad (56c)$$

$$|N_2^u| \approx \begin{pmatrix} 2.03\times10^{-4} & 2.07\times10^{-5} & 6.54\times10^{-2} \\ 3.18\times10^{-8} & 1.32\times10^{-1} & 7.33\times10^{-1} \\ 7.59\times10^{-7} & 5.53\times10^{-3} & 2.92\times10^{-3} \end{pmatrix}. \quad (56d)$$

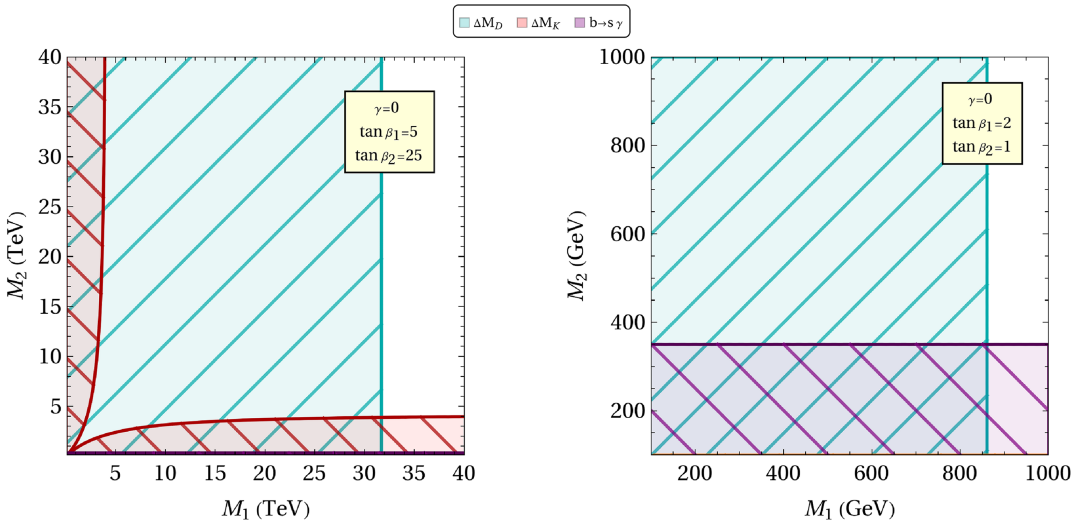


FIG. 2. Constraints from flavor data for the case of $\gamma = 0$ with $\tan\beta_1 = 5$, $\tan\beta_2 = 25$ (left), and $\tan\beta_1 = 2$, $\tan\beta_2 = 1$ (right). The shaded region is forbidden by ΔM_D (cyan), ΔM_K (red), and $b \to s\gamma$ (purple). No additional constraints arise from $\Delta M_{B_{s,d}}$ for the displayed range of parameters. Please note that the ranges are different in the axes of the two plots.

For a second benchmark ($\tan\beta_1 = 2$, $\tan\beta_2 = 1$) implying $v_1 \approx 78$ GeV, $v_2 \approx 156$ GeV, and $v_3 \approx 174$ GeV, which follows a mild hierarchy $v_1 < v_2 < v_3$, we will have

$$|N_1^d| \approx \begin{pmatrix} 5.74\times10^{-5} & 0 & 0 \\ 0 & 2.87\times10^{-4} & 0 \\ 0 & 0 & 0 \end{pmatrix}, \tag{57a}$$

$$|N_2^d| \approx \begin{pmatrix} 2.03\times10^{-5} & 0 & 0 \\ 0 & 4.06\times10^{-4} & 0 \\ 0 & 0 & 1.71\times10^{-2} \end{pmatrix}, \tag{57b}$$

$$|N_1^u| \approx \begin{pmatrix} 2.15\times10^{-5} & 4.09\times10^{-3} & 2.09\times10^{-2} \\ 6.30\times10^{-6} & 2.76\times10^{-3} & 1.64\times10^{-2} \\ 2.42\times10^{-7} & 1.24\times10^{-4} & 6.91\times10^{-4} \end{pmatrix}, \tag{57c}$$

$$|N_2^u| \approx \begin{pmatrix} 8.13\times10^{-6} & 1.65\times10^{-6} & 5.23\times10^{-3} \\ 2.54\times10^{-9} & 5.27\times10^{-3} & 5.86\times10^{-2} \\ 6.06\times10^{-8} & 4.42\times10^{-4} & 6.98\times10^{-1} \end{pmatrix}. \tag{57d}$$

As we can explicitly see from Eqs. (56) and (57), the nonstandard Yukawa couplings are much stronger in the case when $v_1 \ll v_2 \ll v_3$. Therefore, if we wish to safeguard relatively light nonstandard scalars against the flavor constraints, we will need to relax the strong VEV hierarchy.

We will analyze the flavor constraints in the alignment limit defined in Eq. (9). In addition, to ensure automatic compatibility with the theoretical constraints from unitarity [25,26] and boundedness from below [27], we impose the following relations[8]:

$$m_{H_1} = m_{A_1} = m_{C_1} \equiv M_1, \qquad m_{H_2} = m_{A_2} = m_{C_2} \equiv M_2,$$
$$\alpha_3 = \gamma_1 = \gamma_2 \equiv \gamma. \tag{58}$$

Because of the above relations, the custodial symmetry will be embodied by the scalar potential, and therefore the constraints arising from the electroweak T-parameter will also be automatically satisfied [29].

We analyze the constraints arising from neutral meson oscillations, namely ΔM_K, ΔM_{B_s}, ΔM_{B_d}, and ΔM_D, as well as from $b \to s\gamma$.[9] We will focus on the leading order new physics contributions to these processes and use the relevant expressions and methodologies from Refs. [30–33]. First we will address the constraints stemming from $D_0 - \overline{D_0}$ mixing which occurs at the tree level due to the off-diagonal elements $(N^u_{1,2})_{12}$ and $(N^u_{1,2})_{21}$. From Eq. (56) we can see that $(N^u_1)_{12}$ is particularly large for $\tan\beta_{1,2} \gg 1$, a fact that can be easily understood from the explicit expression in Eq. (54a). Consequently, it is preferable to selectively decouple one tier of nonstandard scalars, and arrange γ such that N^u_1 couples predominantly to these decoupled scalars. Based on this strategy, we present benchmark scenarios that largely follow this assumption, with $M_1 \gg M_2$ along with $\gamma \approx 0$.

To showcase the flavor constraints for $v_1 \ll v_2 \ll v_3$, we begin by setting the benchmark at $\tan\beta_1 \approx 5$ and $\tan\beta_2 \approx 25$, and investigating the bounds on M_1 and M_2. As already discussed, we set $\gamma = 0$ to explicitly see that the

[8]Under these convenient assumptions the scalar potential in Eq. (3) will reduce to the maximally symmetric form [3,28].

[9]Please refer to Appendix B for the detailed expressions.

$D_0 - \overline{D_0}$ mixing still allows the second tier of scalars to remain light while M_1 is required to be much heavier than the TeV scale. Interestingly, no additional constraints arise from the B_s and B_d systems. However, $K^0 - \overline{K^0}$ prevents M_2 from being arbitrarily light, as shown in the left panel of Fig. 2. For the benchmark $\tan\beta_1 \approx 5$ and $\tan\beta_2 \approx 25$ the strength of the FCNC interactions becomes substantial [see Eq. (56)], pushing the nonstandard mass scales to large values to satisfy the flavor constraints. Specifically, from the left panel of Fig. 2 we observe that even after selectively

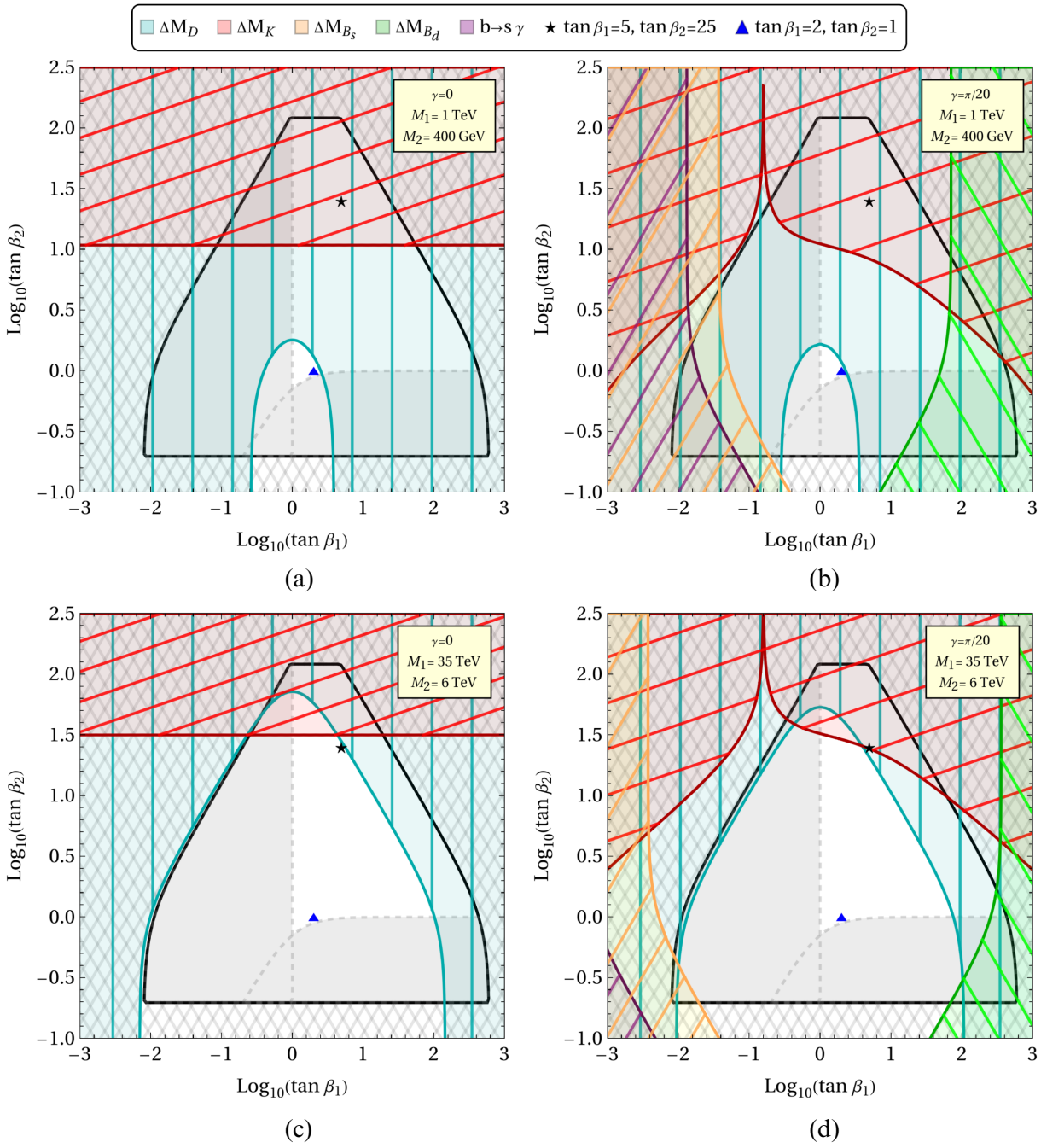


FIG. 3. Flavor data constraints on the $\tan\beta_1$-$\tan\beta_2$ plane for different benchmarks of masses and mixing. The regions shaded and crossed out are excluded due to ΔM_D (cyan), ΔM_K (red), ΔM_{B_s} (orange), ΔM_{B_d} (green), and $b \to s\gamma$ (purple). The perturbative region shown in Fig. 1 is overlaid, with the region outside the black boundary being nonperturbative. The light-gray regions are actually allowed from perturbativity, but correspond to $v_1 > v_2$ (left) and $v_2 > v_3$ (bottom right). The star pinpoints the value $\tan\beta_1 = 5$ and $\tan\beta_2 = 25$, whereas the blue triangle marks the $\tan\beta_1 = 2$, $\tan\beta_2 = 1$ point. (a) $M_1 = 1$ TeV, $M_2 = 400$ GeV, and $\gamma = 0$. (b) $M_1 = 1$ TeV, $M_2 = 400$ GeV, and $\gamma = \pi/20$. (c) $M_1 = 35$ TeV, $M_2 = 6$ TeV, and $\gamma = 0$. (d) $M_1 = 35$ TeV, $M_2 = 6$ TeV, and $\gamma = \pi/20$.

decoupling M_1, M_2 needs to be heavier than $\mathcal{O}(5\ \text{TeV})$ to avoid conflicts with ΔM_K. On the other hand, if we work with a milder VEV hierarchy, $v_1 < v_2 < v_3$, reflected by the benchmark $\tan\beta_1 \approx 2$ and $\tan\beta_2 \approx 1$, then nonstandard masses below the TeV scale can be easily accommodated as can be seen from the right panel of Fig. 2. For this benchmark, the constraint from $b \to s\gamma$ places the lower bound on M_2 ($\gtrsim$350 GeV) as the constraint from $K^0 - \overline{K^0}$ is absent.

We will now cast these bounds in the $\tan\beta_1$-$\tan\beta_2$ plane to illustrate the extent to which the flavor constraints exclude regions of the allowed parameter space shown in Fig. 1. As previously noted, it is not mandatory to have $M_1, M_2 \gg v$ to satisfy the flavor constraints. By relaxing the hierarchy between the VEVs, the model can still accommodate nonstandard scalars below the TeV scale, as showcased in Figs. 3(a) and 3(b). In these figures, we observe that even for masses as light as $M_1 = 1$ TeV and $M_2 = 400$ GeV, the flavor constraints can be successfully satisfied in the unshaded region characterized by $\tan\beta_{1,2} \approx \mathcal{O}(1)$, which corresponds to a relatively mild VEV hierarchy $v_1 < v_2 < v_3$. The differences between Figs. 3(a) and 3(b) highlight the fact that even a small mixing can significantly affect the allowed parameter space. However, if we insist on a stronger VEV hierarchy, $v_1 \ll v_2 \ll v_3$, then the flavor constraints will force the nonstandard masses to be much heavier than the electroweak scale. This is clearly illustrated in Figs. 3(c) and 3(d) where it is evident that the nonstandard masses must lie well above the TeV scale so that the benchmark $\tan\beta_1 = 5$, $\tan\beta_2 = 25$ may be accommodated within the allowed region. Even in this case, it is important to choose $\gamma \approx 0$ to minimize the impact of the flavor constraints.

IV. SUMMARY

BGL-3HDMs feature intriguing Yukawa textures, where the kth generation of the left-handed fermion doublets couple exclusively to the kth scalar doublet. This behavior, together with the observed hierarchical quark masses and mixings, allows the primary sources of mass for different generations of fermions to be disentangled. The distinction between generations, made possible by the flavor symmetry, becomes particularly evident by the $U(1)_1 \times U(1)_2$ realization of the model. Notably, this disentanglement of mass sources does not introduce additional parameters stemming purely from the Yukawa sector. In the version of the model considered here, the Yukawa matrices in the down-quark and charged lepton sectors are manifestly diagonal, simplifying the phenomenology. This lack of off-diagonal elements eliminates tree-level FCNCs in these sectors, and the Yukawa couplings can be directly related to the physical masses leading to a more straightforward interpretation. All the tree-level FCNC interactions mediated by neutral nonstandard Higgses, in the current model, are confined to the up-quark sector only. Moreover, $\tan\beta_1$ and $\tan\beta_2$ are the only new Beyond-Standard-Model parameters that appear in the expressions for $N_{1,2}^{u,d,\ell}$. This particular feature makes these models as predictive as the NFC versions of 3HDM with a $U(1)_1 \times U(1)_2$ symmetry.

Contrary to our initial impressions, the flavor constraints turned out to be very strong for the up-type BGL-3HDM considered here. For the desired VEV hierarchy $v_1 \ll v_2 \ll v_3$, the constraints from neutral meson mixings forbid nonstandard masses below $\mathcal{O}(5\ \text{TeV})$. To allow nonstandard scalars in the sub-TeV regime, we need to relax the aesthetic appeal of maintaining the hierarchy $v_1 \ll v_2 \ll v_3$, i.e., $\tan\beta_{1,2} \gg 1$. This is a direct consequence of the fact that the strength of the tree-level FCNC interactions in the up-quark sector are proportional to the up-type masses. In retrospect, we believe the down-type BGL-3HDM has a relatively better chance of accommodating the flavor constraints. This is because, in the down-type BGL-3HDM case, the tree-level FCNC couplings in the down-quark sector are proportional to the down-type quark masses.

To summarize, despite the strong constraints from the flavor observables, BGL-3HDMs are not without aesthetic appeal. The fact that the bounds on the nonstandard scalar masses are pushed upwards if we insist on diluting the hierarchies among the Yukawa parameters follows directly from the predictive nature of the FCNC matrices. The presence of flavor-diagonal yet nonuniversal couplings in certain fermionic sectors stands out as a key feature of this scenario. This offers a promising avenue for future exploration, particularly if signs of flavor nonuniversality emerge in upcoming data.

ACKNOWLEDGMENTS

D. D. thanks the Anusandhan National Research Foundation (ANRF), India, for financial support through Grant No. CRG/2022/000565. A. M. P. acknowledges support from the University Grants Commission, Government of India, through the SRF fellowship scheme.

DATA AVAILABILITY

The data are not publicly available. The data are available from the authors upon reasonable request.

APPENDIX A: SCALAR SECTOR DETAILS

The scalar potential presented in Eq. (3) involves 15 parameters. The bilinear coefficients m_{11}^2, m_{22}^2, and m_{33}^2 can be replaced by the three VEVs, v_1, v_2, and v_3 or equivalently by v, $\tan\beta_1$, and $\tan\beta_2$. The remaining 12 parameters—comprising nine quartic couplings and three soft-breaking parameters—can be mapped onto the seven physical masses (three CP-even scalars, two CP-odd scalars, and two pairs of charged scalars) and five mixing angles (three in the CP-even sector, one in the CP-odd

sector, and one in the charged scalar sector). The details of this procedure are provided below.

The minimization conditions used to replace the bilinear parameters in terms of the VEVs are given by

$$m_{11}^2 = -\lambda_1 v_1^2 - \frac{1}{2}\{(\lambda_4+\lambda_7)v_2^2 + (\lambda_5+\lambda_8)v_3^2\} + m_{12}^2\frac{v_2}{v_1} + m_{13}^2\frac{v_3}{v_1}, \tag{A1a}$$

$$m_{22}^2 = -\lambda_2 v_2^2 - \frac{1}{2}\{(\lambda_4+\lambda_7)v_1^2 + (\lambda_6+\lambda_9)v_3^2\} + m_{12}^2\frac{v_1}{v_2} + m_{23}^2\frac{v_3}{v_2}, \tag{A1b}$$

$$m_{33}^2 = -\lambda_3 v_3^2 - \frac{1}{2}\{(\lambda_5+\lambda_8)v_1^2 + (\lambda_6+\lambda_9)v_2^2\} + m_{13}^2\frac{v_1}{v_3} + m_{23}^2\frac{v_2}{v_3}. \tag{A1c}$$

Now let us demonstrate the diagonalization of the mass matrices in different sectors following the same prescription as in [20] but in the presence of the soft terms.

1. *CP*-odd scalar sector

The mass terms for the *CP*-odd scalars can be extracted from the scalar potential as

$$V_{\rm PS}^{\rm mass} = \begin{pmatrix} z_1 & z_2 & z_3 \end{pmatrix}\frac{\mathcal{M}_P^2}{2}\begin{pmatrix} z_1 \\ z_2 \\ z_3 \end{pmatrix}, \tag{A2}$$

where $\mathcal{M}_P^2$ is the mass matrix in the Lagrangian basis. It can be block diagonalized by the rotation $\mathcal{O}_\beta$, defined in Eq. (7), as follows:

$$(\mathcal{B}_P)^2 \equiv \mathcal{O}_\beta\cdot\mathcal{M}_P^2\cdot\mathcal{O}_\beta^T = \begin{pmatrix} 0 & 0 & 0 \\ 0 & (\mathcal{B}_P^2)_{22} & (\mathcal{B}_P^2)_{23} \\ 0 & (\mathcal{B}_P^2)_{23} & (\mathcal{B}_P^2)_{33} \end{pmatrix}. \tag{A3a}$$

The elements of the block diagonal matrix are given by

$$(\mathcal{B}_P^2)_{22} = \frac{m_{12}^2(v_1^2+v_2^2)^2 + v_3(m_{23}^2 v_1^3 + m_{13}^2 v_2^3)}{v_1 v_2(v_1^2+v_2^2)}, \tag{A3b}$$

$$(\mathcal{B}_P^2)_{23} = \frac{v(m_{13}^2 v_2 - m_{23}^2 v_1)}{(v_1^2+v_2^2)}, \tag{A3c}$$

$$(\mathcal{B}_P^2)_{33} = -\frac{v^2(m_{13}^2 v_1 + m_{23}^2 v_2)}{(v_1^2+v_2^2)v_3}. \tag{A3d}$$

Further, the matrix $\mathcal{B}_P^2$ can be diagonalized by an orthogonal rotation $\mathcal{O}_{\gamma_1}$ as follows:

$$\mathcal{O}_{\gamma_1}\cdot(\mathcal{B}_P)^2\cdot\mathcal{O}_{\gamma_1}^T = \mathrm{diag}(0, m_{A_1}^2, m_{A_2}^2), \tag{A4}$$

where $\mathcal{O}_{\gamma_1}$ is defined as

$$\mathcal{O}_{\gamma_1} = \begin{pmatrix} 1 & 0 & 0 \\ 0 & \cos\gamma_1 & -\sin\gamma_1 \\ 0 & \sin\gamma_1 & \cos\gamma_1 \end{pmatrix}. \tag{A5}$$

This gives us the following relations:

$$m_{A_1}^2\cos^2\gamma_1 + m_{A_2}^2\sin^2\gamma_1 = (\mathcal{B}_P^2)_{22}, \tag{A6a}$$

$$\cos\gamma_1\sin\gamma_1(m_{A_2}^2 - m_{A_1}^2) = (\mathcal{B}_P^2)_{23}, \tag{A6b}$$

$$m_{A_1}^2\sin^2\gamma_1 + m_{A_2}^2\cos^2\gamma_1 = (\mathcal{B}_P^2)_{33}. \tag{A6c}$$

Additionally, we define the following dimensionless quantities to reparametrize the soft breakings:

$$s_{12} = \frac{2m_{12}^2}{v_1 v_2}, \qquad s_{13} = \frac{2m_{13}^2}{v_1 v_3}, \qquad s_{23} = \frac{2m_{23}^2}{v_2 v_3}. \tag{A7a}$$

Using Eqs. (A3) and (A6) we can solve for s_{12}, s_{13}, and s_{23} as

$$s_{12} = \frac{m_{A_1}^2 + m_{A_2}^2}{2v^2}\left(\frac{1}{c_{\beta_2}^2} - \frac{s_{\beta_2}^2}{c_{\beta_2}^2} + 1\right) + \frac{m_{A_1}^2 - m_{A_2}^2}{2v^2}\left(-\frac{c_{2\beta_2}c_{\gamma_1}^2}{c_{\beta_2}^2} + \frac{3c_{\gamma_1}^2}{c_{\beta_2}^2} - \frac{s_{\beta_2}^2 s_{\gamma_1}^2}{c_{\beta_2}^2} - \frac{3s_{\gamma_1}^2}{c_{\beta_2}^2} - \frac{2c_{2\beta_1}s_{\beta_2}s_{2\gamma_1}}{c_{\beta_1}c_{\beta_2}^2 s_{\beta_1}} + s_{\gamma_1}^2\right), \tag{A8a}$$

$$s_{13} = \frac{m_{A_1}^2 + m_{A_2}^2}{v^2} + \frac{m_{A_1}^2 - m_{A_2}^2}{v^2}\left(-c_{\gamma_1}^2 - \frac{s_{\beta_1}s_{2\gamma_1}}{c_{\beta_1}s_{\beta_2}} + s_{\gamma_1}^2\right), \tag{A8b}$$

$$s_{23} = \frac{m_{A_1}^2 + m_{A_2}^2}{v^2} + \frac{m_{A_1}^2 - m_{A_2}^2}{v^2}\left(-c_{\gamma_1}^2 + \frac{c_{\beta_1}s_{2\gamma_1}}{s_{\beta_1}s_{\beta_2}} + s_{\gamma_1}^2\right). \tag{A8c}$$

2. Charged scalar sector

Similar to the pseudoscalar sector case, the charged scalar sector mass matrix $\mathcal{M}_C^2$ can be block diagonalized as

$$(\mathcal{B}_C)^2 \equiv \mathcal{O}_\beta\cdot\mathcal{M}_C^2\cdot\mathcal{O}_\beta^T = \begin{pmatrix} 0 & 0 & 0 \\ 0 & (\mathcal{B}_C^2)_{22} & (\mathcal{B}_C^2)_{23} \\ 0 & (\mathcal{B}_C^2)_{23} & (\mathcal{B}_C^2)_{33} \end{pmatrix}, \tag{A9a}$$

where

$$(\mathcal{B}_C^2)_{22} = \frac{1}{2(v_1^2+v_2^2)}(s_{23}v_3^2v_1^2 + s_{12}(v_1^2+v_2^2)^2 + s_{13}v_2^2v_3^2 - \lambda_7 v_1^4 - 2\lambda_7 v_2^2v_1^2 - \lambda_9 v_3^2v_1^2 - \lambda_7 v_2^4 - \lambda_8 v_2^2v_3^2), \tag{A9b}$$

$$(\mathcal{B}_C^2)_{23} = \frac{v_1v_2v_3}{2(v_1^2+v_2^2)}v(s_{13} - s_{23} - \lambda_8 + \lambda_9), \tag{A9c}$$

$$(\mathcal{B}_C^2)_{33} = \frac{v^2}{2(v_1^2+v_2^2)}(+s_{13}v_1^2 + s_{23}v_2^2 - \lambda_8 v_1^2 - \lambda_9 v_2^2). \tag{A9d}$$

Further, the charged scalar mass matrix can be completely diagonalized with the use of the rotation matrix $\mathcal{O}_{\gamma_2}$ as

$$\mathcal{O}_{\gamma_2}\cdot(\mathcal{B}_C)^2\cdot\mathcal{O}_{\gamma_2}^T = \mathrm{diag}(0, m_{C_1}^2, m_{C_2}^2), \tag{A10}$$

where $\mathcal{O}_{\gamma_2}$ is defined as

$$\mathcal{O}_{\gamma_2} = \begin{pmatrix} 1 & 0 & 0 \\ 0 & \cos\gamma_2 & -\sin\gamma_2 \\ 0 & \sin\gamma_2 & \cos\gamma_2 \end{pmatrix}. \tag{A11}$$

Doing so, we get the following relations:

$$m_{C_1}^2\cos^2\gamma_2 + m_{C_2}^2\sin^2\gamma_2 = (\mathcal{B}_C^2)_{22}, \tag{A12a}$$

$$\cos\gamma_2\sin\gamma_2(m_{C_2}^2 - m_{C_1}^2) = (\mathcal{B}_C^2)_{23}, \tag{A12b}$$

$$m_{C_1}^2\sin^2\gamma_2 + m_{C_2}^2\cos^2\gamma_2 = (\mathcal{B}_C^2)_{33}. \tag{A12c}$$

These equations in conjunction with Eq. (A9) will enable us to solve for λ_7, λ_8, and λ_9 as given below:

$$\lambda_7 = s_{12} - \frac{m_{C_1}^2 + m_{C_2}^2}{v^2} + \frac{m_{C_1}^2 - m_{C_2}^2}{2v^2}\times\left(\frac{c_{2\beta_2}c_{2\gamma_2}}{c_{\beta_2}^2} - \frac{3c_{2\gamma_2}}{c_{\beta_2}^2} + \frac{2c_{2\beta_1}s_{\beta_2}s_{2\gamma_2}}{c_{\beta_1}c_{\beta_2}^2 s_{\beta_1}}\right), \tag{A13a}$$

$$\lambda_8 = s_{13} + \frac{m_{C_1}^2}{v^2}\left(\frac{s_{\beta_1}s_{2\gamma_2}}{c_{\beta_1}s_{\beta_2}} - 2s_{\gamma_2}^2\right) - \frac{m_{C_2}^2}{v^2}\left(2c_{\gamma_2}^2 + \frac{s_{\beta_1}s_{2\gamma_2}}{c_{\beta_1}s_{\beta_2}}\right), \tag{A13b}$$

$$\lambda_9 = s_{23} - \frac{m_{C_1}^2}{v^2}\left(\frac{c_{\beta_1}s_{2\gamma_2}}{s_{\beta_1}s_{\beta_2}} + 2s_{\gamma_2}^2\right) + \frac{m_{C_2}^2}{v^2}\left(\frac{c_{\beta_1}s_{2\gamma_2}}{s_{\beta_1}s_{\beta_2}} - 2c_{\gamma_2}^2\right), \tag{A13c}$$

where the expressions for s_{12}, s_{13}, and s_{23} can be replaced using Eq. (A8).

3. *CP*-even scalar sector

The mass terms of the *CP*-even scalars in the Lagrangian basis can be extracted from the potential as

$$V_S^{\mathrm{mass}} = \begin{pmatrix} h_1 & h_2 & h_3 \end{pmatrix}\frac{\mathcal{M}_S^2}{2}\begin{pmatrix} h_1 \\ h_2 \\ h_3 \end{pmatrix}, \tag{A14a}$$

where $\mathcal{M}_S^2$ is the mass matrix whose elements are as follows:

$$(\mathcal{M}_S^2)_{11} = \frac{1}{2}(s_{12}v_2^2 + s_{13}v_3^2 + 4\lambda_1 v_1^2), \tag{A14b}$$

$$(\mathcal{M}_S^2)_{12} = v_1v_2\left(-\frac{1}{2}s_{12} + \lambda_4 + \lambda_7\right), \tag{A14c}$$

$$(\mathcal{M}_S^2)_{13} = v_1v_3\left(-\frac{1}{2}s_{13} + \lambda_5 + \lambda_8\right), \tag{A14d}$$

$$(\mathcal{M}_S^2)_{22} = \frac{1}{2}(s_{12}v_1^2 + s_{23}v_3^2 + 4\lambda_2 v_2^2), \tag{A14e}$$

$$(\mathcal{M}_S^2)_{23} = v_2v_3\left(-\frac{1}{2}s_{23} + \lambda_6 + \lambda_9\right), \tag{A14f}$$

$$(\mathcal{M}_S^2)_{33} = \frac{1}{2}(s_{13}v_1^2 + s_{23}v_2^2 + 4\lambda_3 v_3^2). \tag{A14g}$$

This mass matrix can be diagonalized by the following orthogonal rotation:

$$\mathcal{O}_\alpha\cdot\mathcal{M}_S^2\cdot\mathcal{O}_\alpha^T \equiv \begin{pmatrix} m_h^2 & 0 & 0 \\ 0 & m_{H_1}^2 & 0 \\ 0 & 0 & m_{H_2}^2 \end{pmatrix}, \tag{A15}$$

where $\mathcal{O}_\alpha$ is defined as follows:

$$\mathcal{O}_\alpha = \mathcal{R}_3\cdot\mathcal{R}_2\cdot\mathcal{R}_1, \tag{A16a}$$

with[10]

$$\mathcal{R}_1 = \begin{pmatrix} c_{\alpha_1} & s_{\alpha_1} & 0 \\ -s_{\alpha_1} & c_{\alpha_1} & 0 \\ 0 & 0 & 1 \end{pmatrix}, \qquad \mathcal{R}_2 = \begin{pmatrix} c_{\alpha_2} & 0 & s_{\alpha_2} \\ 0 & 1 & 0 \\ -s_{\alpha_2} & 0 & c_{\alpha_2} \end{pmatrix},$$
$$\mathcal{R}_3 = \begin{pmatrix} 1 & 0 & 0 \\ 0 & c_{\alpha_3} & -s_{\alpha_3} \\ 0 & s_{\alpha_3} & c_{\alpha_3} \end{pmatrix}. \tag{A16b}$$

Inverting Eq. (A15),

[10]It should be noted that our definition of α_3 differs from that in Ref. [20] by a negative sign.

$$\mathcal{M}_S^2 \equiv \mathcal{O}_\alpha^T \cdot \begin{pmatrix} m_h^2 & 0 & 0 \\ 0 & m_{H_1}^2 & 0 \\ 0 & 0 & m_{H_2}^2 \end{pmatrix} \cdot \mathcal{O}_\alpha, \tag{A17}$$

which can be solved to obtain the remaining six λ_i as follows:

$$\lambda_1 = -\frac{s_{12}s_{\beta_1}^2}{4c_{\beta_1}^2} - \frac{s_{13}s_{\beta_2}^2}{4c_{\beta_1}^2c_{\beta_2}^2} + \frac{c_{\alpha_1}^2c_{\alpha_2}^2m_h^2}{2v^2c_{\beta_1}^2c_{\beta_2}^2} + \frac{m_{H_1}^2}{v^2}\left(\frac{c_{\alpha_3}^2s_{\alpha_1}^2}{2c_{\beta_1}^2c_{\beta_2}^2} + \frac{c_{\alpha_1}^2s_{\alpha_2}^2s_{\alpha_3}^2}{2c_{\beta_1}^2c_{\beta_2}^2} - \frac{s_{2\alpha_1}s_{\alpha_2}s_{2\alpha_3}}{4c_{\beta_1}^2c_{\beta_2}^2}\right) + \frac{m_{H_2}^2}{v^2}\left(\frac{c_{\alpha_1}^2c_{\alpha_3}^2s_{\alpha_2}^2}{2c_{\beta_1}^2c_{\beta_2}^2} + \frac{c_{\alpha_1}c_{\alpha_3}s_{\alpha_1}s_{\alpha_3}s_{\alpha_2}}{c_{\beta_1}^2c_{\beta_2}^2} + \frac{s_{\alpha_1}^2s_{\alpha_3}^2}{2c_{\beta_1}^2c_{\beta_2}^2}\right), \tag{A18a}$$

$$\lambda_2 = -\frac{s_{12}c_{\beta_1}^2}{4s_{\beta_1}^2} - \frac{s_{23}s_{\beta_2}^2}{4c_{\beta_2}^2s_{\beta_1}^2} + \frac{c_{\alpha_2}^2m_h^2s_{\alpha_1}^2}{2v^2c_{\beta_2}^2s_{\beta_1}^2} + \frac{m_{H_1}^2}{v^2}\left(\frac{c_{\alpha_1}^2c_{\alpha_3}^2}{2c_{\beta_2}^2s_{\beta_1}^2} + \frac{c_{\alpha_1}c_{\alpha_3}s_{\alpha_1}s_{\alpha_2}s_{\alpha_3}}{c_{\beta_2}^2s_{\beta_1}^2} + \frac{s_{\alpha_1}^2s_{\alpha_2}^2s_{\alpha_3}^2}{2c_{\beta_2}^2s_{\beta_1}^2}\right) + \frac{m_{H_2}^2}{v^2}\left(\frac{c_{\alpha_3}^2s_{\alpha_1}^2s_{\alpha_2}^2}{2c_{\beta_2}^2s_{\beta_1}^2} - \frac{s_{2\alpha_1}s_{2\alpha_3}s_{\alpha_2}}{4c_{\beta_2}^2s_{\beta_1}^2} + \frac{c_{\alpha_1}^2s_{\alpha_3}^2}{2c_{\beta_2}^2s_{\beta_1}^2}\right), \tag{A18b}$$

$$\lambda_3 = -\frac{s_{13}c_{\beta_1}^2c_{\beta_2}^2}{4s_{\beta_2}^2} - \frac{s_{23}c_{\beta_2}^2s_{\beta_1}^2}{4s_{\beta_2}^2} + \frac{m_h^2s_{\alpha_2}^2}{2v^2s_{\beta_2}^2} + \frac{m_{H_1}^2}{v^2}\left(\frac{c_{\alpha_2}^2}{4s_{\beta_2}^2} - \frac{c_{\alpha_2}^2c_{2\alpha_3}}{4s_{\beta_2}^2}\right) + \frac{m_{H_2}^2}{v^2}\left(\frac{c_{2\alpha_3}c_{\alpha_2}^2}{4s_{\beta_2}^2} + \frac{c_{\alpha_2}^2}{4s_{\beta_2}^2}\right), \tag{A18c}$$

$$\lambda_4 = \frac{s_{12}}{2} - \lambda_7 + \frac{c_{\alpha_2}^2m_h^2s_{2\alpha_1}}{2v^2c_{\beta_1}c_{\beta_2}^2s_{\beta_1}} + \frac{m_{H_1}^2}{v^2}\left(-\frac{c_{\alpha_2}^2s_{2\alpha_1}}{4c_{\beta_1}c_{\beta_2}^2s_{\beta_1}} + \frac{c_{2\alpha_1}s_{\alpha_2}s_{2\alpha_3}}{2c_{\beta_1}c_{\beta_2}^2s_{\beta_1}} + \frac{c_{2\alpha_2}c_{2\alpha_3}s_{2\alpha_1}}{8c_{\beta_1}c_{\beta_2}^2s_{\beta_1}} - \frac{3c_{2\alpha_3}s_{2\alpha_1}}{8c_{\beta_1}c_{\beta_2}^2s_{\beta_1}}\right) + \frac{m_{H_2}^2}{v^2}\left(-\frac{c_{\alpha_2}^2s_{2\alpha_1}}{4c_{\beta_1}c_{\beta_2}^2s_{\beta_1}} - \frac{c_{2\alpha_1}s_{\alpha_2}s_{2\alpha_3}}{2c_{\beta_1}c_{\beta_2}^2s_{\beta_1}} - \frac{c_{2\alpha_2}c_{2\alpha_3}s_{2\alpha_1}}{8c_{\beta_1}c_{\beta_2}^2s_{\beta_1}} + \frac{3c_{2\alpha_3}s_{2\alpha_1}}{8c_{\beta_1}c_{\beta_2}^2s_{\beta_1}}\right), \tag{A18d}$$

$$\lambda_5 = \frac{s_{13}}{2} - \lambda_8 + \frac{c_{\alpha_1}m_h^2s_{2\alpha_2}}{2v^2c_{\beta_1}c_{\beta_2}s_{\beta_2}} + \frac{m_{H_1}^2}{v^2}\left(-\frac{c_{\alpha_1}s_{2\alpha_2}}{4c_{\beta_1}c_{\beta_2}s_{\beta_2}} + \frac{c_{\alpha_1}c_{2\alpha_3}s_{2\alpha_2}}{4c_{\beta_1}c_{\beta_2}s_{\beta_2}} + \frac{c_{\alpha_2}s_{\alpha_1}s_{2\alpha_3}}{2c_{\beta_1}c_{\beta_2}s_{\beta_2}}\right) + \frac{m_{H_2}^2}{v^2}\left(-\frac{c_{\alpha_1}s_{2\alpha_2}}{4c_{\beta_1}c_{\beta_2}s_{\beta_2}} - \frac{c_{\alpha_1}c_{2\alpha_3}s_{2\alpha_2}}{4c_{\beta_1}c_{\beta_2}s_{\beta_2}} - \frac{c_{\alpha_2}s_{\alpha_1}s_{2\alpha_3}}{2c_{\beta_1}c_{\beta_2}s_{\beta_2}}\right), \tag{A18e}$$

$$\lambda_6 = \frac{s_{23}}{2} - \lambda_9 + \frac{m_h^2s_{\alpha_1}s_{2\alpha_2}}{v^2s_{\beta_1}s_{2\beta_2}} + \frac{m_{H_1}^2}{v^2}\left(\frac{c_{2\alpha_3}s_{\alpha_1}s_{2\alpha_2}}{2s_{\beta_1}s_{2\beta_2}} - \frac{c_{\alpha_1}c_{\alpha_2}s_{2\alpha_3}}{2c_{\beta_2}s_{\beta_1}s_{\beta_2}} - \frac{s_{\alpha_1}s_{2\alpha_2}}{2s_{\beta_1}s_{2\beta_2}}\right) + \frac{m_{H_2}^2}{v^2}\left(-\frac{c_{\alpha_3}^2s_{\alpha_1}s_{2\alpha_2}}{2c_{\beta_2}s_{\beta_1}s_{\beta_2}} + \frac{c_{\alpha_1}c_{\alpha_2}s_{2\alpha_3}}{2c_{\beta_2}s_{\beta_1}s_{\beta_2}}\right). \tag{A18f}$$

Substituting s_{ij} from Eq. (A8) and λ_7, λ_8, λ_9 from Eq. (A13), we obtain expressions for the remaining λ_i in terms of the chosen set of parameters.

APPENDIX B: EXPRESSIONS FOR THE FLAVOR OBSERVABLES

1. Computing $b \to s\gamma$

In the absence of down-quark sector FCNCs, the nonstandard contributions to the $b \to s\gamma$ amplitude come from the charged scalar mediated diagrams shown in Fig. 4.

In what follows, we first present the analysis used for an NFC 3HDM in Ref. [3] and then adapt the results for complex and nonuniversal charged-Higgs couplings. As per Ref. [34], the branching ratio for $b \to s\gamma$ is controlled by the C_{7L}^{eff} and C_{7R}^{eff} Wilson coefficients:

$$\frac{\text{Br}(b \to s\gamma)}{\text{Br}(b \to ce\bar{\nu})} = \frac{6\alpha}{\pi B}\left|\frac{V_{ts}^*V_{tb}}{V_{cb}}\right|^2[|C_{7L}^{\text{eff}}|^2 + |C_{7R}^{\text{eff}}|^2], \tag{B1}$$

where the normalization by $\text{Br}(b \to ce\bar{\nu})$ cancels some of the hadronic uncertainties. Further, the effective Wilson coefficients read

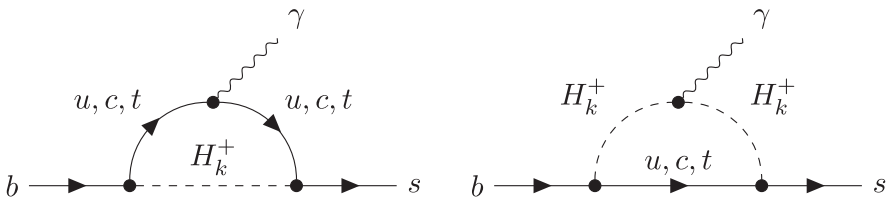


FIG. 4. New physics contributions to $b \to s\gamma$ in the up-type BGL-3HDM.

$$C_{7L}^{\text{eff}} = \eta^{16/23} C_{7L} + \frac{8}{3}(\eta^{14/23} - \eta^{16/23}) C_{8L} + \sum_{i=1}^{8} h_i \eta^{a_i}, \tag{B2a}$$

$$C_{7R}^{\text{eff}} = \eta^{16/23} C_{7R} + \frac{8}{3}(\eta^{14/23} - \eta^{16/23}) C_{8R}, \tag{B2b}$$

where, as in the usual analysis of 2HDMs [34], the leading log QCD corrections in the SM are described by

$$a_i = \left(\tfrac{14}{23},\ \tfrac{16}{23},\ \tfrac{6}{23},\ -\tfrac{12}{23},\ 0.4086,\ -0.4230,\ -0.8994,\ 0.1456\right), \tag{B2c}$$

$$h_i = \left(\tfrac{626126}{272277},\ -\tfrac{56281}{51730},\ -\tfrac{3}{7},\ -\tfrac{1}{14},\ -0.6494,\ -0.0380,\ -0.0185,\ -0.0057\right), \tag{B2d}$$

and $\eta = \alpha_s(M_Z)/\alpha_s(m_b)$, where m_b is the mass of the bottom quark. Taking into account the absence of tree-level FCNCs, the coefficients C_{7L} and C_{7R} in Eqs. (B2a) and (B2b) can be written as

$$C_{7L} = A_\gamma^{\text{SM}} + A_{\gamma L}^{+}, \qquad C_{7R} = \frac{m_s}{m_b} A_\gamma^{\text{SM}} + A_{\gamma R}^{+}, \tag{B3a}$$

$$C_{8L} = A_g^{\text{SM}} + A_{gL}^{+}, \qquad C_{8R} = \frac{m_s}{m_b} A_g^{\text{SM}} + A_{gR}^{+}, \tag{B3b}$$

where the superscripts "SM" and "+" denote the SM contributions and the charged-Higgs contributions, respectively. These contributions can be further broken down into

$$A_{\gamma L,R}^{+} = \frac{1}{V_{ts}^* V_{tb}} \sum_{q=u,c,t} V_{qs}^* V_{qb} \sum_{k=1,2} \left[C_{1L,R}^k(y_q^k) + \frac{2}{3} C_{2L,R}^k(y_q^k) \right], \tag{B4a}$$

$$A_{gL,R}^{+} = \frac{1}{V_{ts}^* V_{tb}} \sum_{q=u,c,t} V_{qs}^* V_{qb} \sum_{k=1,2} C_{2L,R}^k(y_q^k), \tag{B4b}$$

with $y_q^k = m_q^2/M_{H_k^+}^2$, where the index k runs over the charged-Higgses and the index q runs over the up-quarks in the loop. The coefficients $C_{1L,R}^k$ and $C_{2L,R}^k$ in the NFC 3HDM case are expressed as

$$C_{1L,R}^k(y_q) = \frac{y_q}{4} \left\{ \left[\overline{\mathcal{F}_2}(y_q) - \overline{\mathcal{F}_1}(y_q) \right] \left(\frac{m_{s,b}^2}{m_q^2} Y_k^2 + X_k^2 \right) + 2 X_k Y_k \left[\overline{\mathcal{F}_1}(y_q) - \overline{\mathcal{F}_0}(y_q) \right] \right\}, \tag{B5a}$$

$$C_{2L,R}^k(y_q) = \frac{y_q}{4} \left\{ \left[\mathcal{F}_2(y_q) - \mathcal{F}_1(y_q) \right] \left(\frac{m_{s,b}^2}{m_q^2} Y_k^2 + X_k^2 \right) - 2 X_k Y_k \mathcal{F}_1(y_q) \right\}, \tag{B5b}$$

where the values of the numbers X_k and Y_k are defined with respect to the charged-Goldstone couplings. More explicitly, since the charged Goldstone couples to quarks in the following manner:

$$\mathcal{L}_{G^\pm}^{Q} = \frac{\sqrt{2}}{v} G^+ \bar{u} [(D_u V) P_L - (V D_d) P_R] d + \text{H.c.}, \tag{B6}$$

the values of X_k and Y_k are extracted from the charged-Higgs coupling as

$$\mathcal{L}^{Q}_{H_1^\pm} = \frac{\sqrt{2}}{v} H_1^+ \bar{u}[X_1(D_u V)P_L + Y_1(VD_d)P_R]d + \text{H.c.}, \tag{B7a}$$

$$\mathcal{L}^{Q}_{H_2^\pm} = \frac{\sqrt{2}}{v} H_2^+ \bar{u}[X_2(D_u V)P_L + Y_2(VD_d)P_R]d + \text{H.c.} \tag{B7b}$$

The loop functions are given by

$$\mathcal{F}_n(t) = \int_0^1 dx \frac{(1-x)^n}{x+(1-x)t} = \frac{1}{(n+1)t} {}_2F_1\left(1,1;n+2;\frac{t-1}{t}\right), \tag{B8a}$$

$$\bar{\mathcal{F}}_n(t) = \int_0^1 dx \frac{x^n}{x+(1-x)t} = \frac{1}{(n+1)t} {}_2F_1\left(1,n+1;n+2;\frac{t-1}{t}\right), \tag{B8b}$$

where ${}_pF_q(a,b;c;d)$ is the hypergeometric function. Finally, the SM amplitude is given by (keeping only the top contribution)

$$A_\gamma^{\text{SM}} = \left[\frac{(2-3x_t)}{2}\overline{\mathcal{F}_1}(x_t) + \frac{(2+x_t)}{2}\overline{\mathcal{F}_2}(x_t) + x_t\bar{\mathcal{F}}_0(x_t) + \frac{4}{3}\mathcal{F}_0(x_t) - \frac{(6-x_t)}{3}\mathcal{F}_1(x_t) + \frac{(2+x_t)}{3}\mathcal{F}_2(x_t)\right] - \frac{23}{36}, \tag{B9a}$$

$$A_g^{\text{SM}} = \left[2\mathcal{F}_0(x_t) - \frac{(6-x_t)}{2}\mathcal{F}_1(x_t) + \frac{(2+x_t)}{2}\mathcal{F}_2(x_t)\right] - \frac{1}{3}, \tag{B9b}$$

where $x_t = m_t^2/M_W^2$. So far, we have presented the analysis of the $b \to s\gamma$ processes in a NFC 3HDM as given in Ref. [3].

To extend these results to our model, we redefine Eq. (B5) to allow for complex values of X_k and Y_k and also allow them to be different for different flavors of the quarks that are involved. The numbers X_k and Y_k in the mass basis can be obtained from the corresponding numbers X'_k and Y'_k in the intermediate basis [see Eq. (6)] by means of the basis rotation described in Eq. (8). Since the charged-Higgses $H'^\pm_k$ in the intermediate basis couple to quarks as per equation Eq. (25), we can extract X'_k and Y'_k for the interaction between up-quark q and down-quark β as follows:

$$(X'_k)_{q\beta} = \frac{v(N_k^{u\dagger}V)_{q\beta}}{m_q V_{q\beta}}, \quad (Y'_k)_{q\beta} = -\frac{v(VN_k^d)_{q\beta}}{m_\beta V_{q\beta}}, \tag{B10}$$

where the indices $k = 1, 2$ are for the charged-Higgses, $q = u, c, t$ for the up-type quarks, and $\beta = d, s, b$ for the down-type quarks. With these additions, the analogs of coefficients expressed in Eq. (B5), now named as $C^{k,q}_{1L,R}$ and $C^{k,q}_{2L,R}$, can be expressed as

$$C^{k,q}_{1L,R}(y_q) = \frac{y_q}{4}\left\{\left[\overline{\mathcal{F}_2}(y_q) - \overline{\mathcal{F}_1}(y_q)\right] \times \left(\frac{m^2_{s,b}}{m_q^2}(Y_k)_{qb}(Y_k)^*_{qs} + (X_k)_{qb}(X_k)^*_{qs}\right) + \left[\overline{\mathcal{F}_1}(y_q) - \overline{\mathcal{F}_0}(y_q)\right]((X_k)_{qb}(Y_k)^*_{qs} + (X_k)^*_{qs}(Y_k)_{qb})\right\}, \tag{B11a}$$

$$C^{k,q}_{2L,R}(y_q) = \frac{y_q}{4}\left\{\left[\mathcal{F}_2(y_q) - \mathcal{F}_1(y_q)\right] \times \left(\frac{m^2_{s,b}}{m_q^2}(Y_k)_{qb}(Y_k)^*_{qs} + (X_k)_{qb}(X_k)^*_{qs}\right) - \mathcal{F}_1(y_q)((X_k)_{qb}(Y_k)^*_{qs} + (X_k)^*_{qs}(Y_k)_{qb})\right\}. \tag{B11b}$$

Finally, the SM prediction for the $b \to s\gamma$ branching ratio can be found in Ref. [35]. The experimental values of $b \to s\gamma$ and $b \to ce\nu$ branching ratios can be found in Ref. [23] and combined as prescribed in Eq. (B1) with their errors added in quadrature to obtain the 2σ allowed region.

2. Neutral meson oscillations

In this part of the appendix, we lay out all the necessary details to compute the meson oscillation parameter for a nHDM. In practice, this provides a generalization of the results found in Ref. [30], to a scenario with more than one charged scalars. For clarity and ease of reading, we list the set of conventions used in this appendix:

(i) The meson P^0 is the bound state of the quarks $(\bar{q}_1 q_2)$, with q_1 and q_2 having the same electric charge.
(ii) The indices k, k_1, k_2 run through neutral scalars, whereas i, j cover the charged scalars.
(iii) The indices a, b refer to the quarks with electric charge different from q_1 and q_2 (up quarks for down-type mesons and down quarks for up-type mesons). Conversely, c, d refer to the quarks of the same electric charge as q_1 and q_2.

(iv) To avoid any possible confusion with q_1 and q_2, the quarks in the loops with indices a, b or c, d are represented by f.
(v) $\Gamma(n+1) = n!$ is the usual Gamma function.
(vi) The vertices for the Yukawa and $W_\mu^\pm$ interactions are defined as

$$\mathscr{L}_{\rm int} = \bar{\psi}_i(\Gamma^L_{\bar{\psi}_i\psi_j\varphi_k}P_L + \Gamma^R_{\bar{\psi}_i\psi_j\varphi_k}P_R)\psi_j\varphi_k + \bar{\psi}_i(\Gamma^L_{\bar{\psi}_i\psi_j W^\pm}\gamma^\mu P_L)\psi_j W^\pm_\mu, \tag{B12}$$

where $P_{L,R}$ are the usual projection operators and ψ (φ) can refer to any fermion (scalar) field. Although we write it in a simplified notation, $\mathscr{L}_{\rm int}$ must respect all the symmetries of the theory, as well as be Hermitian, and therefore vertices require the fields $\psi_{i,j}$ and φ_k to respect charge conservation.

The relevant effective Hamiltonian for $\Delta F = 2$ processes is given by

$$\mathcal{H}^{\Delta F=2}_{\rm eff} = \sum_{i=1}^{5} C_i O_i + \sum_{i=1}^{3} C'_i O'_i + \text{H.c.}, \tag{B13}$$

where we work in the same operator basis as Refs. [30,36]:

$$\begin{aligned} O_1 &= (\bar{q}_1^\alpha\gamma^\mu P_L q_2^\alpha)(\bar{q}_1^\beta\gamma_\mu P_L q_2^\beta), \quad O_2 = (\bar{q}_1^\alpha P_L q_2^\alpha)(\bar{q}_1^\beta P_L q_2^\beta), \\ O_3 &= (\bar{q}_1^\alpha P_L q_2^\beta)(\bar{q}_1^\beta P_L q_2^\alpha), \quad O_4 = (\bar{q}_1^\alpha P_L q_2^\alpha)(\bar{q}_1^\beta P_R q_2^\beta), \\ O_5 &= (\bar{q}_1^\alpha P_L q_2^\beta)(\bar{q}_1^\beta P_R q_2^\alpha), \end{aligned} \tag{B14}$$

where α and β denote color indices and the primed operators can be found by the interchange $L \leftrightarrow R$. We note that $C_3 = 0$ for all the diagrams computed (tree-level diagrams and box diagrams), but C_5 is generally nonzero, although it couples different color indices in each invariant combination. Although the couplings to the scalars and W_μ bosons do not give rise to this operator directly, they may induce other operators that are related to O_5 through Fierz transformations, such as [37]

$$\begin{aligned} (\bar{q}_1^\alpha\gamma_\mu P_R q_2^\alpha)(\bar{q}_1^\beta\gamma_\mu P_L q_2^\beta) &= -2(\bar{q}_1^\alpha P_L q_2^\beta)(\bar{q}_1^\beta P_R q_2^\alpha) \\ &= -2O_5. \end{aligned} \tag{B15}$$

The ensuing contribution to ΔM_P is

$$\Delta M_P = \left| -\frac{1}{M_P} C_i \langle \bar{P}^0|O_i|P^0\rangle \right|, \tag{B16}$$

where the matrix elements are defined as [38,39]

$$\begin{aligned} \langle \bar{P}^0|O_1|P^0\rangle &= \xi_1 B_1 M_P^2 f_P^2, \\ \langle \bar{P}^0|O_i|P^0\rangle &= \xi_i B_i \left[\frac{M_P^2}{(m_{q_1}+m_{q_2})^2} + d_i\right] M_P^2 f_P^2, \end{aligned} \tag{B17}$$

with $\xi_i = (2/3, -5/12, 1/12, 1/2, 1/6)$, whereas $d_4 = 1/6$, $d_5 = 3/2$, and $d_{1,2,3} = 0$, with B_i being the Bag parameters [39,40]. The decay constants f_P have been taken from [41].

Before we present the Wilson coefficients, we can define the two relevant loop functions:

$$g_1(m_1,m_2,m_3,m_4) = -\frac{m_1 \log m_1}{(m_1-m_2)(m_1-m_3)(m_1-m_4)}, \tag{B18a}$$

$$f_1(m_1,m_2,m_3,m_4) = g_1(m_1,m_2,m_3,m_4) + (m_1 \leftrightarrow m_2) + (m_1 \leftrightarrow m_3) + (m_1 \leftrightarrow m_4), \tag{B18b}$$

$$g_2(m_1,m_2,m_3,m_4) = \frac{1}{2}\frac{m_1^2 \log m_1}{(m_1-m_2)(m_1-m_3)(m_1-m_4)}, \tag{B18c}$$

$$f_2(m_1,m_2,m_3,m_4) = g_2(m_1,m_2,m_3,m_4) + (m_1 \leftrightarrow m_2) + (m_1 \leftrightarrow m_3) + (m_1 \leftrightarrow m_4). \tag{B18d}$$

As usual, degenerate cases need to be handled with care, as these functions have well-defined limits for the cases where $m_i = m_j$.

The new physics contributions to the Wilson coefficients arise from different types of diagrams, shown in Fig. 5. Below, we single out the contributions to the different Wilson coefficients arising from each type of diagram.

Tree-level diagrams

The tree-level contributions coming from nondiagonal N^d and N^u matrices follow from diagrams represented in Fig. 5(a). The Wilson coefficients stemming from these diagrams are

$$C_2 = \sum_k \frac{-1}{2M^2_{S^0_k}}(\Gamma^L_{\bar{q}_1 q_2 S^0_k})^2, \qquad C'_2 = \sum_k \frac{-1}{2M^2_{S^0_k}}(\Gamma^R_{\bar{q}_1 q_2 S^0_k})^2,$$
$$C_4 = \sum_k \frac{-1}{M^2_{S^0_k}}(\Gamma^L_{\bar{q}_1 q_2 S^0_k}\Gamma^R_{\bar{q}_1 q_2 S^0_k}). \tag{B19}$$

Gauge-charged diagrams

The contributions from box diagrams with one gauge boson and one charged Higgs, as shown in Fig. 5(b), are

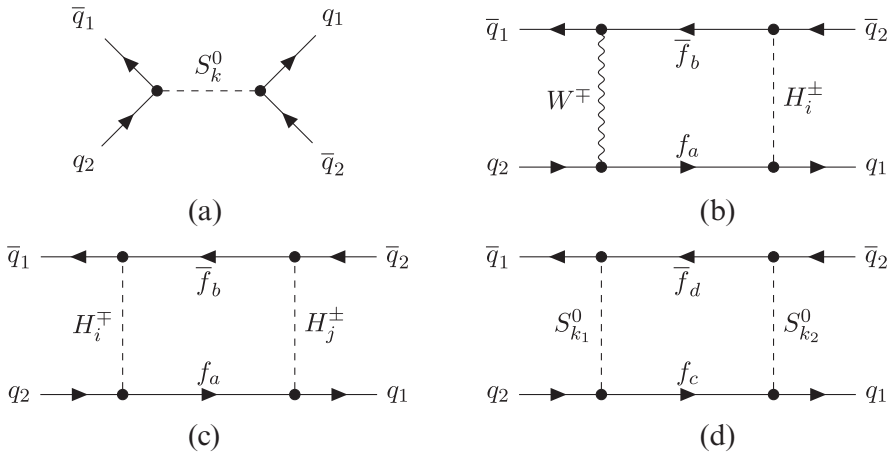


FIG. 5. New physics contributions to ΔM_P. (a) Tree-level diagrams. (b) Gauge-charged diagrams. (c) Charged-Higgs box diagrams. (d) Charged-Higgs box diagrams.

$$C_1 = \frac{1}{16\pi^2}\frac{\Gamma(4)}{6}\sum_i\sum_{a,b}(\Gamma^L_{\bar{q}_1 f_a W^\mp})(\Gamma^L_{q_2\bar{f}_b W^\pm})(\Gamma^L_{q_2\bar{f}_b H_i^\pm})(\Gamma^R_{\bar{q}_1 f_a H_i^\mp})m_a m_b f_1(M_W^2, M_{H_i^\pm}^2, m_a^2, m_b^2), \tag{B20a}$$

$$C_4 = \frac{-1}{16\pi^2}\frac{\Gamma(4)}{3}\sum_i\sum_{a,b}(\Gamma^L_{\bar{q}_1 f_a W^\mp})(\Gamma^L_{q_2\bar{f}_b W^\pm})(\Gamma^R_{q_2\bar{f}_b H_i^\pm})(\Gamma^L_{\bar{q}_1 f_a H_i^\mp})f_2(M_W^2, M_{H_i^\pm}^2, m_a^2, m_b^2). \tag{B20b}$$

Charged-charged box diagrams

The diagrams in Fig. 5(c), which have two charged scalars in the loop, contribute as (the primed coefficients can be found by taking the replacement $L \leftrightarrow R$)

$$C_1 = \frac{1}{16\pi^2}\frac{\Gamma(4)}{24}\sum_{i,j}\sum_{a,b}(\Gamma^R_{\bar{q}_1 f_a H_i^\mp})(\Gamma^L_{\bar{f}_a q_2 H_j^\pm})(\Gamma^R_{\bar{q}_1 f_b H_j^\mp})(\Gamma^L_{q_2\bar{f}_b H_i^\pm})f_2(M_{H_j^\pm}^2, M_{H_j^\pm}^2, m_a^2, m_b^2), \tag{B21a}$$

$$C_2 = \frac{-1}{16\pi^2}\frac{\Gamma(4)}{12}\sum_{i,j}\sum_{a,b}(\Gamma^L_{\bar{q}_1 f_a H_i^\mp})(\Gamma^L_{\bar{f}_a q_2 H_j^\pm})(\Gamma^L_{\bar{q}_1 f_b H_j^\mp})(\Gamma^L_{q_2\bar{f}_b H_i^\pm})m_a m_b f_1(M_{H_i^\pm}^2, M_{H_j^\pm}^2, m_a^2, m_b^2), \tag{B21b}$$

$$C_4 = \frac{-1}{8\pi^2}\frac{\Gamma(4)}{12}\sum_{i,j}\sum_{a,b}(\Gamma^L_{\bar{q}_1 f_a H_i^\mp})(\Gamma^L_{\bar{f}_a q_2 H_j^\pm})(\Gamma^R_{\bar{q}_1 f_b H_j^\mp})(\Gamma^R_{q_2\bar{f}_b H_i^\pm})m_a m_b f_1(M_{H_i^\pm}^2, M_{H_j^\pm}^2, m_a^2, m_b^2), \tag{B21c}$$

$$C_5 = \frac{-1}{8\pi^2}\frac{\Gamma(4)}{12}\sum_{i,j}\sum_{a,b}(\Gamma^R_{\bar{q}_1 f_a H_i^\mp})(\Gamma^L_{\bar{f}_a q_2 H_j^\pm})(\Gamma^L_{\bar{q}_1 f_b H_j^\mp})(\Gamma^R_{q_2\bar{f}_b H_i^\pm})f_2(M_{H_i^\pm}^2, M_{H_j^\pm}^2, m_a^2, m_b^2). \tag{B21d}$$

Neutral Higgs box diagrams

Finally, the neutral box diagrams of Fig. 5(d) amount to ($C'_{1,2,3} = C_{1,2,3}$ with $L \leftrightarrow R$)

$$C_1 = \frac{1}{16\pi^2}\frac{\Gamma(4)}{24}\sum_{k_1,k_2}\sum_{c,d}(\Gamma^R_{\bar{q}_1 f_c S^0_{k_1}})(\Gamma^L_{q_2\bar{f}_c S^0_{k_2}})(\Gamma^R_{\bar{q}_1 f_d S^0_{k_2}})(\Gamma^L_{q_2\bar{f}_d S^0_{k_1}})f_2(M^2_{S^0_{k_1}}, M^2_{S^0_{k_2}}, m_c^2, m_d^2), \tag{B22a}$$

$$C_2 = \frac{-1}{16\pi^2}\frac{\Gamma(4)}{12}\sum_{k_1,k_2}\sum_{c,d}(\Gamma^L_{\bar{q}_1 f_c S^0_{k_1}})(\Gamma^L_{q_2\bar{f}_c S^0_{k_2}})(\Gamma^L_{\bar{q}_1 f_d S^0_{k_2}})(\Gamma^L_{q_2\bar{f}_d S^0_{k_1}})m_c m_d f_1(M^2_{S^0_{k_1}}, M^2_{S^0_{k_2}}, m_c^2, m_d^2), \tag{B22b}$$

$$C_4 = \frac{-1}{8\pi^2}\frac{\Gamma(4)}{12}\sum_{k_1,k_2}\sum_{c,d}(\Gamma^L_{\bar{q}_1 f_c S^0_{k_1}})(\Gamma^L_{q_2\bar{f}_c S^0_{k_2}})(\Gamma^R_{\bar{q}_1 f_d S^0_{k_2}})(\Gamma^R_{q_2\bar{f}_d S^0_{k_1}})m_c m_d f_1(M^2_{S^0_{k_1}}, M^2_{S^0_{k_2}}, m_c^2, m_d^2), \tag{B22c}$$

$$C_5 = \frac{-1}{8\pi^2}\frac{\Gamma(4)}{12}\sum_{k_1,k_2}\sum_{c,d}(\Gamma^R_{\bar{q}_1 f_c S^0_{k_1}})(\Gamma^L_{q_2\bar{f}_c S^0_{k_2}})(\Gamma^L_{\bar{q}_1 f_d S^0_{k_2}})(\Gamma^R_{q_2\bar{f}_d S^0_{k_1}})f_2(M^2_{S^0_{k_1}}, M^2_{S^0_{k_2}}, m_c^2, m_d^2). \tag{B22d}$$

a. Explicit formulas for the vertices in terms of N_k^u and N_k^d

The expressions given above for the Wilson coefficients rely on building the Lagrangian in the physical basis and extracting the expressions for the vertices. However, as we have seen in the main text, for nHDMs it is quite useful to define the matrices that govern the FCNCs: N_k^u and N_k^d. These matrices can be defined in a Higgs basis, and although the actual vertices with the physical eigenstates will depend on a linear combination of N_k, they can already give intuitive knowledge on the model. As such, we provide here the expressions for the relevant vertices for $\Delta F = 2$ transitions in terms of N_k^u and N_k^d.

We start by rewriting the Yukawa Lagrangian in the Higgs basis:

$$\begin{aligned}\mathscr{L}_Y =& -\bar{d}D_d d - \bar{u}D_u u - \frac{H_0}{v}(\bar{d}D_d d + \bar{u}D_u u)\\ &- i\frac{G^0}{v}(\bar{d}D_d\gamma_5 d - \bar{u}D_u\gamma_5 u)\\ &- \sqrt{2}\frac{G^+}{v}\bar{u}[-(D_u V)P_L + (VD_d)P_R]d\\ &- \sqrt{2}\frac{G^-}{v}\bar{d}[(D_d V^\dagger)P_L + (V^\dagger D_u)P_R]u\\ &- R_k[\bar{d}(N_k^d P_R + (N_k^d)^\dagger P_L)d + \bar{u}(N_k^u P_R + (N_k^u)^\dagger P_L)u]\\ &- iA'_k[\bar{d}(N_k^d P_R - (N_k^d)^\dagger P_L)d - \bar{u}(N_k^u P_R - (N_k^u)^\dagger P_L)u]\\ &- \sqrt{2}H'^+_k\bar{u}[VN_k^d P_R - (N_k^u)^\dagger V P_L]d\\ &- \sqrt{2}H'^-_k\bar{d}[-V^\dagger N_k^u P_R + (N_k^d)^\dagger V^\dagger P_L]u. \end{aligned} \tag{B23}$$

Since the Higgs basis already singles out the Goldstones, we can relate the physical eigenstates and the Higgs basis states in full generality via

$$\begin{pmatrix} G^+ \\ H_k^+ \end{pmatrix} = \begin{pmatrix} 1 & 0 \\ 0 & R_C \end{pmatrix}\begin{pmatrix} G^+ \\ H'^+_k \end{pmatrix},$$
$$\begin{pmatrix} G^0 \\ A_k \\ h \\ H_k \end{pmatrix} = \begin{pmatrix} 1 & 0 & \\ 0 & R_A & R_X \\ & R'_X & R_H \end{pmatrix}\begin{pmatrix} G^0 \\ A'_k \\ H_0 \\ R_k \end{pmatrix}, \tag{B24}$$

where, for an nHDM, both R_C and R_A are $(n-1)\times(n-1)$ matrices, R_H is $n\times n$, and last, R_X^T and R'_X are $n\times(n-1)$ matrices. In the limit where CP is conserved in the scalar potential, an identification of CP-even and CP-odd scalar fields is possible, and thus R_X and R'_X vanish. Furthermore, the alignment limit corresponds to $(R_H)_{11} = 1$, which ensures the identification of the 125 GeV scalar, h, with the SM-like Higgs field, H_0.

For completeness, we present the explicit forms of the vertices relevant to the ΔM_P computation, expressed in terms of the Higgs basis matrices N_k^u and N_k^d from Eq. (B23), whose specific expressions in our model are given in Eq. (22). We also express the vertices in terms of the rotation matrices defined in Eq. (B24), which, in the particular case considered in the main text, take the form:

$$\begin{aligned} &R_X = 0, \qquad R'_X = 0, \qquad R_H = O_\alpha O_\beta^T,\\ &R_A = O_{\gamma_1}, \qquad R_C = O_{\gamma_2}, \end{aligned} \tag{B25}$$

where the relevant matrices are defined in Eqs. (7) and (8). The vertices for the h field, which in the alignment limit become flavor diagonal, are given by

$$\begin{aligned}\Gamma^L_{\bar{d}_\alpha d_\beta h} =& -\{(R_H^\dagger)_{k+1,1} - i[(R'_X)^\dagger]_{k,1}\}[(N_k^d)^\dagger]_{\alpha\beta}\\ &- (R_H^\dagger)_{11}\frac{(D_d)_{\alpha\beta}}{v}, \end{aligned} \tag{B26a}$$

$$\begin{aligned}\Gamma^R_{\bar{d}_\alpha d_\beta h} =& -\{(R_H^\dagger)_{k+1,1} + i[(R'_X)^\dagger]_{k,1}\}(N_k^d)_{\alpha\beta}\\ &- (R_H^\dagger)_{11}\frac{(D_d)_{\alpha\beta}}{v}, \end{aligned} \tag{B26b}$$

$$\begin{aligned}\Gamma^L_{\bar{u}_\alpha u_\beta h} =& -\{(R_H^\dagger)_{k+1,1} + i[(R'_X)^\dagger]_{k,1}\}[(N_k^u)^\dagger]_{\alpha\beta}\\ &- (R_H^\dagger)_{11}\frac{(D_u)_{\alpha\beta}}{v}, \end{aligned} \tag{B26c}$$

$$\begin{aligned}\Gamma^R_{\bar{u}_\alpha u_\beta h} =& -\{(R_H^\dagger)_{k+1,1} - i[(R'_X)^\dagger]_{k,1}\}(N_k^u)_{\alpha\beta}\\ &- (R_H^\dagger)_{11}\frac{(D_u)_{\alpha\beta}}{v}. \end{aligned} \tag{B26d}$$

The charged-Higgs interactions, responsible for the leading-order contribution in sectors without tree-level FCNCs, are

$$\begin{aligned}\Gamma^L_{\bar{d}_\alpha u_\beta H_j^-} &= -\sqrt{2}(R_C)_{j,k}[(N_k^d)^\dagger V^\dagger]_{\alpha\beta},\\ \Gamma^R_{\bar{d}_\alpha u_\beta H_j^-} &= \sqrt{2}(R_C)_{j,k}[V^\dagger N_k^u]_{\alpha\beta}, \end{aligned} \tag{B27a}$$

$$\begin{aligned}\Gamma^L_{\bar{u}_\alpha d_\beta H_j^+} &= \sqrt{2}(R_C^\dagger)_{k,j}[(N_k^u)^\dagger V]_{\alpha\beta},\\ \Gamma^R_{\bar{d}_\alpha u_\beta H_j^-} &= -\sqrt{2}(R_C^\dagger)_{k,j}[VN_k^d]_{\alpha\beta}. \end{aligned} \tag{B27b}$$

Finally, the couplings to the remaining neutral scalars, which in the alignment limit will provide the tree-level contributions if $N_k^{u,d}$ are nondiagonal, and will also be responsible for the neutral box diagrams, are given by

$$\begin{aligned}\Gamma^L_{\bar{d}_\alpha d_\beta H_j} =& -\{(R_H^\dagger)_{k+1,j+1} - i[(R'_X)^\dagger]_{k,j+1}\}[(N_k^d)^\dagger]_{\alpha\beta}\\ &- (R_H^\dagger)_{1,j+1}\frac{(D_d)_{\alpha\beta}}{v}, \end{aligned} \tag{B28a}$$

$$\Gamma^{R}_{\bar{d}_\alpha d_\beta H_j} = -\{(R_H^\dagger)_{k+1,j+1} + i[(R'_X)^\dagger]_{k,j+1}\}(N_k^d)_{\alpha\beta} - (R_H^\dagger)_{1,j+1}\frac{(D_d)_{\alpha\beta}}{v}, \tag{B28b}$$

$$\Gamma^{L}_{\bar{u}_\alpha u_\beta H_j} = -\{(R_H^\dagger)_{k+1,j+1} + i[(R'_X)^\dagger]_{k,j+1}\}[(N_k^u)^\dagger]_{\alpha\beta} - (R_H^\dagger)_{1,j+1}\frac{(D_u)_{\alpha\beta}}{v}, \tag{B28c}$$

$$\Gamma^{R}_{\bar{u}_\alpha u_\beta H_j} = -\{(R_H^\dagger)_{k+1,j+1} - i[(R'_X)^\dagger]_{k,j+1}\}(N_k^u)_{\alpha\beta} - (R_H^\dagger)_{1,j+1}\frac{(D_u)_{\alpha\beta}}{v}, \tag{B28d}$$

for the H_j fields, whereas for A_j we find

$$\Gamma^{L}_{\bar{d}_\alpha d_\beta A_j} = -\{(R_X^\dagger)_{k+1,j} - i(R_A^\dagger)_{k,j}\}[(N_k^d)^\dagger]_{\alpha\beta} - (R_X^\dagger)_{1,j}\frac{(D_d)_{\alpha\beta}}{v}, \tag{B29a}$$

$$\Gamma^{R}_{\bar{d}_\alpha d_\beta A_j} = -\{(R_X^\dagger)_{k+1,j} + i(R_A^\dagger)_{k,j}\}(N_k^d)_{\alpha\beta} - (R_X^\dagger)_{1,j}\frac{(D_d)_{\alpha\beta}}{v} \tag{B29b}$$

$$\Gamma^{L}_{\bar{u}_\alpha u_\beta A_j} = -\{(R_X^\dagger)_{k+1,j} + i(R_A^\dagger)_{k,j}\}[(N_k^u)^\dagger]_{\alpha\beta} - (R_X^\dagger)_{1,j}\frac{(D_u)_{\alpha\beta}}{v}, \tag{B29c}$$

$$\Gamma^{R}_{\bar{u}_\alpha u_\beta A_j} = -\{(R_X^\dagger)_{k+1,j} - i(R_A^\dagger)_{k,j}\}(N_k^u)_{\alpha\beta} - (R_X^\dagger)_{1,j}\frac{(D_u)_{\alpha\beta}}{v}. \tag{B29d}$$

In the spirit of completeness, we show below the explicit expressions taking both the limit of CP conservation and the alignment limit. In this case, the flavor-changing couplings ($\alpha \neq \beta$) are given by[11]

$$\Gamma^{L}_{\bar{d}_\alpha d_\beta H_j} = -(R_H^\dagger)_{k+1,j+1}[(N_k^d)^\dagger]_{\alpha\beta},$$
$$\Gamma^{L}_{\bar{d}_\alpha d_\beta A_j} = i(R_A^\dagger)_{k,j}[(N_k^d)^\dagger]_{\alpha\beta}, \tag{B30a}$$

$$\Gamma^{R}_{\bar{d}_\alpha d_\beta H_j} = -(R_H^\dagger)_{k+1,j+1}(N_k^d)_{\alpha\beta},$$
$$\Gamma^{R}_{\bar{d}_\alpha d_\beta A_j} = -i(R_A^\dagger)_{k,j}(N_k^d)_{\alpha\beta}, \tag{B30b}$$

$$\Gamma^{L}_{\bar{u}_\alpha u_\beta H_j} = -(R_H^\dagger)_{k+1,j+1}[(N_k^u)^\dagger]_{\alpha\beta},$$
$$\Gamma^{L}_{\bar{u}_\alpha u_\beta A_j} = -i(R_A^\dagger)_{k,j}[(N_k^u)^\dagger]_{\alpha\beta}, \tag{B30c}$$

$$\Gamma^{R}_{\bar{u}_\alpha u_\beta H_j} = -(R_H^\dagger)_{k+1,j+1}(N_k^u)_{\alpha\beta},$$
$$\Gamma^{R}_{\bar{u}_\alpha u_\beta A_j} = i(R_A^\dagger)_{k,j}(N_k^u)_{\alpha\beta}, \tag{B30d}$$

where we can directly see that having a tier-wise degeneracy between M_{H_j} and A_j, together with the same mixing for the nonstandard CP-even and CP-odd scalars, $(R_H)_{i+1,j+1} = (R_A)_{i,j}$, will provide a cancellation between the scalar and pseudoscalar tree-level contributions to C_2 and C_2', since

$$(\Gamma^{L,R}_{\bar{q}_1 q_2 H_j})^2 = -(\Gamma^{L,R}_{\bar{q}_1 q_2 A_j})^2, \tag{B31}$$

but does not cancel the tree-level contribution to C_4.

[11] The charged-Higgs couplings are unaffected by this limit, and so we do not repeat them.

[1] S. L. Glashow and S. Weinberg, Natural conservation laws for neutral currents, Phys. Rev. D **15**, 1958 (1977).

[2] R. Boto, J. C. Romão, and J. P. Silva, Current bounds on the type-Z Z_3 three-Higgs-doublet model, Phys. Rev. D **104**, 095006 (2021).

[3] M. Chakraborti, D. Das, M. Levy, S. Mukherjee, and I. Saha, Prospects for light charged scalars in a three-Higgs-doublet model with Z_3 symmetry, Phys. Rev. D **104**, 075033 (2021).

[4] R. Boto, D. Das, L. Lourenco, J. C. Romao, and J. P. Silva, Fingerprinting the type-Z three-Higgs-doublet models, Phys. Rev. D **108**, 015020 (2023).

[5] J. a. M. Alves, F. J. Botella, G. C. Branco, and M. Nebot, Extending trinity to the scalar sector through discrete flavoured symmetries, Eur. Phys. J. C **80**, 710 (2020).

[6] W. Altmannshofer and K. Toner, Flavor constraints in a generational three Higgs doublet model, Phys. Rev. D **111**, 075009 (2025).

[7] F. J. Botella, G. C. Branco, and M. N. Rebelo, Minimal flavour violation and multi-Higgs models, Phys. Lett. B **687**, 194 (2010).

[8] H. Serôdio, Yukawa sector of multi Higgs doublet models in the presence of Abelian symmetries, Phys. Rev. D **88**, 056015 (2013).

[9] D. Emmanuel-Costa, J. I. Silva-Marcos, and N. R. Agostinho, Exploring the quark flavor puzzle within the three-Higgs doublet model, Phys. Rev. D **96**, 073006 (2017).
[10] D. Das, P. M. Ferreira, A. P. Morais, I. Padilla-Gay, R. Pasechnik, and J. P. Rodrigues, A three Higgs doublet model with symmetry-suppressed flavour changing neutral currents, J. High Energy Phys. 11 (2021) 079.
[11] G. C. Branco, W. Grimus, and L. Lavoura, Relating the scalar flavor changing neutral couplings to the CKM matrix, Phys. Lett. B **380**, 119 (1996).
[12] J. M. Alves, F. J. Botella, G. C. Branco, F. Cornet-Gomez, and M. Nebot, Controlled flavour changing neutral couplings in two Higgs doublet models, Eur. Phys. J. C **77**, 585 (2017).
[13] I. P. Ivanov, V. Keus, and E. Vdovin, Abelian symmetries in multi-Higgs-doublet models, J. Phys. A **45**, 215201 (2012).
[14] P. M. Ferreira and J. P. Silva, Discrete and continuous symmetries in multi-Higgs-doublet models, Phys. Rev. D **78**, 116007 (2008).
[15] G. Bhattacharyya and D. Das, Nondecoupling of charged scalars in Higgs decay to two photons and symmetries of the scalar potential, Phys. Rev. D **91**, 015005 (2015).
[16] F. Faro, J. C. Romao, and J. P. Silva, Nondecoupling in multi-Higgs doublet models, Eur. Phys. J. C **80**, 635 (2020).
[17] H. Georgi and D. V. Nanopoulos, Suppression of flavor changing effects from neutral spinless meson exchange in gauge theories, Phys. Lett. **82B**, 95 (1979).
[18] L. Lavoura and J. P. Silva, Fundamental *CP* violating quantities in a $\mathrm{SU}(2) \times \mathrm{U}(1)$ model with many Higgs doublets, Phys. Rev. D **50**, 4619 (1994).
[19] S. Davidson and H. E. Haber, Basis-independent methods for the two-Higgs-doublet model, Phys. Rev. D **72**, 035004 (2005); **72**, 099902(E) (2005).
[20] D. Das and I. Saha, Alignment limit in three Higgs-doublet models, Phys. Rev. D **100**, 035021 (2019).
[21] A. Tumasyan *et al.* (CMS Collaboration), A portrait of the Higgs boson by the CMS experiment ten years after the discovery, Nature (London) **607**, 60 (2022); **623**, E4 (2023).
[22] L. Wolfenstein, Parametrization of the Kobayashi-Maskawa matrix, Phys. Rev. Lett. **51**, 1945 (1983).
[23] S. Navas *et al.* (Particle Data Group Collaboration), Review of particle physics, Phys. Rev. D **110**, 030001 (2024).
[24] D. Das, 2HDM without FCNC: Off the beaten tracks, Eur. Phys. J. C **78**, 650 (2018).
[25] D. Das and U. K. Dey, Analysis of an extended scalar sector with S_3 symmetry, Phys. Rev. D **89**, 095025 (2014); **91**, 039905(E) (2015).
[26] M. P. Bento, J. C. Romão, and J. a. P. Silva, Unitarity bounds for all symmetry-constrained 3HDMs, J. High Energy Phys. 08 (2022) 273.
[27] F. S. Faro and I. P. Ivanov, Boundedness from below in the $U(1) \times U(1)$ three-Higgs-doublet model, Phys. Rev. D **100**, 035038 (2019).
[28] N. Darvishi, M. R. Masouminia, and A. Pilaftsis, Maximally symmetric three-Higgs-doublet model, Phys. Rev. D **104**, 115017 (2021).
[29] D. Das, M. Levy, P. B. Pal, A. M. Prasad, I. Saha, and A. Srivastava, Democratic three-Higgs-doublet models: The custodial limit and wrong-sign Yukawa coupling, Phys. Rev. D **107**, 055035 (2023).
[30] A. Crivellin, A. Kokulu, and C. Greub, Flavor-phenomenology of two-Higgs-doublet models with generic Yukawa structure, Phys. Rev. D **87**, 094031 (2013).
[31] F. J. Botella, G. C. Branco, M. Nebot, and M. N. Rebelo, Flavour changing Higgs couplings in a class of two Higgs doublet models, Eur. Phys. J. C **76**, 161 (2016).
[32] G. Bhattacharyya, D. Das, and A. Kundu, Feasibility of light scalars in a class of two-Higgs-doublet models and their decay signatures, Phys. Rev. D **89**, 095029 (2014).
[33] M. Nebot and J. P. Silva, Self-cancellation of a scalar in neutral meson mixing and implications for the LHC, Phys. Rev. D **92**, 085010 (2015).
[34] P. Gambino and M. Misiak, Quark mass effects in anti-$\bar{B} \to X_s\gamma$, Nucl. Phys. **B611**, 338 (2001).
[35] M. Misiak, A. Rehman, and M. Steinhauser, Towards $\bar{B} \to X_s\gamma$ at the NNLO in QCD without interpolation in m_c, J. High Energy Phys. 06 (2020) 175.
[36] M. Ciuchini, E. Franco, V. Lubicz, G. Martinelli, I. Scimemi, and L. Silvestrini, Next-to-leading order QCD corrections to $\Delta\mathrm{F} = 2$ effective Hamiltonians, Nucl. Phys. **B523**, 501 (1998).
[37] A. Buras, *Gauge Theory of Weak Decays* (Cambridge University Press, Cambridge, England, 2020), p. 6.
[38] F. Gabbiani, E. Gabrielli, A. Masiero, and L. Silvestrini, A complete analysis of FCNC and *CP* constraints in general SUSY extensions of the standard model, Nucl. Phys. **B477**, 321 (1996).
[39] A. Bazavov *et al.* (Fermilab Lattice, MILC Collaborations), $B^0_{(s)}$-mixing matrix elements from lattice QCD for the standard model and beyond, Phys. Rev. D **93**, 113016 (2016).
[40] N. Carrasco, P. Dimopoulos, R. Frezzotti, V. Lubicz, G. C. Rossi, S. Simula, and C. Tarantino (ETM Collaboration), $\Delta\mathrm{S} = 2$ and $\Delta\mathrm{C} = 2$ bag parameters in the standard model and beyond from $\mathrm{N}_f = 2 + 1 + 1$ twisted-mass lattice QCD, Phys. Rev. D **92**, 034516 (2015).
[41] Y. Aoki *et al.* (Flavour Lattice Averaging Group (FLAG) Collaboration), FLAG review 2021, Eur. Phys. J. C **82**, 869 (2022).